



# INORGANIC CHEMISTRY

## FRONTIERS



## REVIEW



Cite this: *Inorg. Chem. Front.*, 2016, **3**, 741

Received 25th November 2015,  
Accepted 31st January 2016

DOI: 10.1039/c5qi00262a

rs.c.li/frontiers-inorganic

## Recent developments of iron pincer complexes for catalytic applications

Gerald Bauer and Xile Hu\*

Iron catalysis is attractive for organic synthesis because iron is inexpensive, abundant, and non-toxic. To control the activity and stability of an iron center, a large number of iron pincer complexes have been synthesized. Many such complexes exhibit excellent catalytic activity in a number of important organic reactions such as hydrogenation, hydrosilylation, dehydrogenation, and carbon–carbon bond forming reactions. In this review, recent examples of representative iron pincer catalysts are presented.

### 1. Introduction

Complexes of precious metals, particularly those from the platinum group, occupy a central place in homogeneous catalysis. However, the high cost and potential toxicity of precious metals make them less desirable for industrial applications. Thus, homogeneous catalysis using more abundant and cheaper first row transition metals has become a popular research theme. Iron catalysis is particularly desirable because iron is inexpensive, readily available, and non-toxic. In biological systems iron-containing enzymes are widely used as cata-

lysts, and examples include cytochrome P-450, peroxidases, various oxygenases, and hydrogenases. While numerous reports of iron-catalyzed organic reactions are known,<sup>1,2</sup> studies of well-defined iron catalysts are less common. Such studies, however, are essential for the in-depth understanding and further advancement of iron catalysis.

This review focuses on the catalytic applications of iron pincer complexes.<sup>3,6–8</sup> Pincer ligands, in general, are tridentate, 6-electron donor ligands that enforce a meridional coordination geometry on the metal center. Although there is no strict definition, a pincer ligand traditionally consists of a central benzene ring, which is 1,3-disubstituted with two chelating side arms (Fig. 1). Both the central atom (Dc) and the donors at the two arms (Ds) bind to the metal center, resulting in strong chelation.<sup>4,5,9–15</sup> Replacement of the central aryl ring

Laboratory of Inorganic Synthesis and Catalysis, Institute of Chemical Sciences and Engineering, École Polytechnique Fédérale de Lausanne (EPFL), ISIC-LSCI, BCH 3305, 1015 Lausanne, Switzerland. E-mail: xile.hu@epfl.ch



Gerald Bauer

Gerald Bauer was born in 1984 in Tulln/Donau, Austria. He studied 'Technical Chemistry' at the University of Technology in Vienna with semesters at the UCT in Prague and the University of Waterloo, ON, Canada during his bachelor studies. Gerald received his M.Sc. in 2010 under the joint supervision of Prof. Karl Kirchner, UT Vienna, and Prof. Kazushi Mashima, University of Osaka. Shortly afterwards, he joined the

lab of Prof. Xile Hu at the EPFL working on the catalytic applications and mechanistic investigation of iron pincer complexes in Kumada cross-coupling reactions, for which he was awarded his PhD in 2015.



Xile Hu

Xile Hu was born in 1978 in Putian, China. He received a B.S. degree from Peking University (2000) and a Ph.D. degree from the University of California, San Diego (2004; advisor: Prof. Karsten Meyer). He carried out a postdoctoral study at the California Institute of Technology (advisor: Prof. Jonas Peters) before joining the École Polytechnique Fédérale de Lausanne (EPFL) as a tenure-track assistant professor in 2007. He is currently an associate professor at the same institute. His research interests span from organometallic chemistry, synthetic methodologies, and reaction mechanisms to bio-mimetic and bio-specified coordination chemistry to electrocatalysis and artificial photosynthesis.

lysts, and examples include cytochrome P-450, peroxidases, various oxygenases, and hydrogenases. While numerous reports of iron-catalyzed organic reactions are known,<sup>1,2</sup> studies of well-defined iron catalysts are less common. Such studies, however, are essential for the in-depth understanding and further advancement of iron catalysis.





Fig. 1 Generalized structure of pincer complexes.<sup>3–5</sup>

by a pyridinyl or diarylamine group leads to two major classes of variants of the original pincer ligands. In addition to their strong chelating ability and structural rigidity, the advantage of pincer ligands is their diversity. By modifying the central and side donors as well as the ligand backbone, it is possible to synthesize an almost endless number of ligands with varying electronic and steric properties.<sup>5</sup> This diversity is very attractive for homogeneous catalysis where systematic studies of metal–ligand combinations are desired.

In this review, iron complexes of pincer ligands based on the following frameworks are discussed: 2,6-disubstituted pyridine, 1,3-disubstituted benzene, *N,N*-diarylamine, isoindoline and bis(phosphinoethyl)amine. Only catalysis by pre-formed iron complexes, but not *in situ* generated iron species, will be presented. The examples are selected to give a representative, but not comprehensive overview of the developments in the field. Mostly symmetrically substituted pincer ligands with a  $C_2$  or  $C_{2v}$  symmetry are included. Unsymmetrically substituted ligands and terpyridine-type ligands are not treated. Pyridine diimines (PDI) might be considered as pincer ligands, and

their iron complexes are very active for polymerization,<sup>16–19</sup> hydrogenation, and other alkene, alkyne, and ketone functionalization reactions. Several excellent reviews covering these iron complexes have been published recently.<sup>20,21</sup> Therefore, they will not be reviewed here.

## 2. Neutral pyridine-based PNP ligand systems and their applications in iron catalysis

The first iron PNP complexes were synthesized by Dahlhoff and Nelson in 1971 by reacting 2,6-bis(diphenylphosphino)methylpyridine with  $\text{FeX}_2$  ( $X = \text{Cl}, \text{Br}, \text{I}, \text{NCS}$ ). The resulting complexes were in a high spin configuration and exhibited a 5-coordinate geometry with a slightly distorted square pyramidal structure.<sup>6</sup> This ligand framework became popular, and in addition to the variance of the substituents on the phosphorus donors,<sup>5</sup> the linker ( $L$ ) that connects the phosphorus donors to the central pyridine ring could be modified to include not only  $\text{CR}_2$ ,<sup>6,22–31</sup> but also  $\text{NR}$ <sup>5,32–39</sup> and  $\text{O}$  (Fig. 2).<sup>40,41</sup> To differentiate between the different linkers, these pincer ligands are abbreviated as “ $\text{P}^L\text{N}^L\text{P}$ ”, where  $L = \text{C}, \text{N}, \text{O}$ , to represent  $\text{CR}_2$ ,  $\text{NR}$ , and  $\text{O}$ , respectively.

Several groups studied the influence of linkers on the electronic density of the metal centre using the IR frequencies of  $\text{M–CO}$  bonds as a probe (Fig. 3).<sup>26,34,40</sup> The CO stretching frequency of  $[(\text{PNP})\text{FeX}_2(\text{CO})]$  ( $X = \text{Cl}, \text{Br}$ ) decreases when the



Fig. 2 Structure of pyridine-based PNP ligands and selected chiral and achiral substituents on the phosphorus.<sup>5</sup>

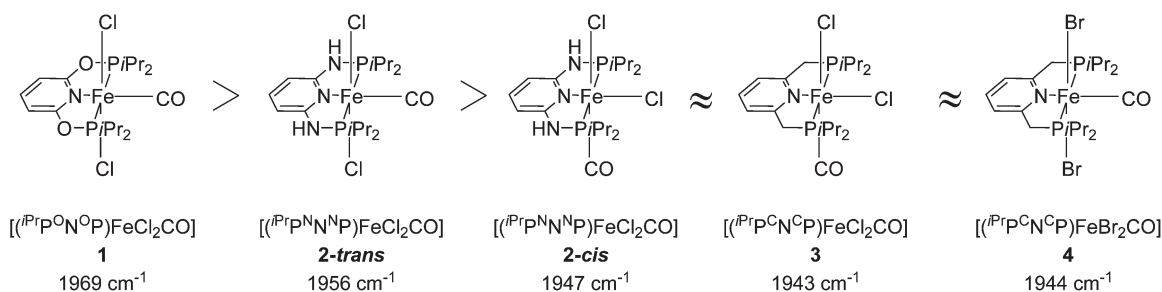


Fig. 3 CO stretching frequencies for **1**, **2-cis**, **2-trans**, **3** and **4**.<sup>26,34,40</sup>



linker is changed from O to NH and to CH<sub>2</sub>. This result suggests that the electron donating character of the corresponding PNP ligands follows a similar order.

An interesting feature of these PNP pincer complexes is their metal–ligand cooperation. The slightly acidic CH<sub>2</sub> and NH linkers are easily deprotonated under basic conditions, which causes a reversible dearomatization of the central pyridine ring.<sup>42</sup> Further details will be discussed below.

## 2.1 Iron(II) P<sup>N</sup>N<sup>N</sup>P pincer complexes for the selective formation of 3-hydroxyacrylates from benzaldehydes and ethyl diazoacetates

Aldehydes react with ethyl diazoacetates (EDA) in the presence of Lewis acids (e.g. BF<sub>3</sub>, ZnCl<sub>2</sub>, AlCl<sub>3</sub>, SnCl<sub>2</sub>, GeCl<sub>2</sub>) to form β-keto esters.<sup>43</sup> It was previously shown that the Lewis acid [(η<sup>5</sup>-Cp)Fe(CO)<sub>2</sub>THF](BF<sub>4</sub>) catalyzed the reaction of benzaldehydes with EDA to give β-hydroxy-2-aryl acrylates.<sup>44,45</sup>

More recently Kirchner and co-workers employed *cis*-[(<sup>i</sup>PrP<sup>N</sup>N<sup>N</sup>P)Fe(CO)(CH<sub>3</sub>CN)<sub>2</sub>](X)<sub>2</sub> (**5-X**; X = BF<sub>4</sub><sup>-</sup>, BArF<sup>-</sup>) for the reaction of *p*-anisaldehyde with EDA (Fig. 4).<sup>33</sup> These reactions produced selectively a hydroxyl acrylate (**A**, >80%) and only trace amounts of a β-keto ester (**B**). The two counter ions, BF<sub>4</sub><sup>-</sup> and BArF<sup>-</sup>, gave similar results. A tentative mechanistic proposal is given in Fig. 5. The CO ligand exhibits a stronger *trans* effect than the nitrogen of the pyridine ring. Therefore the acetonitrile opposite to the carbonyl will be cleaved first. The dissociation of acetonitrile and successive coordination of an aldehyde gives intermediate **6**. The nucleophilic attack of EDA on the C=O bond gives the transition state **7**, which upon elimination of N<sub>2</sub> yields complex **8**. Migration of the aryl substituent then leads to **9**. The newly formed aldehyde is released and tautomerizes into the thermodynamically more stable ethyl 3-hydroxy-2-(4-methoxyphenyl)acrylate.<sup>33</sup>

Kirchner and co-workers then examined the reaction using a series of mono-cationic dicarbonyl complexes *trans*-[(<sup>i</sup>PrP<sup>N</sup>N<sup>N</sup>P)Fe(CO)<sub>2</sub>Cl](X) (**10-X**, X = NO<sub>3</sub><sup>-</sup>, CF<sub>3</sub>COO<sup>-</sup>, CF<sub>3</sub>SO<sub>3</sub><sup>-</sup>, BF<sub>4</sub><sup>-</sup>, PF<sub>6</sub><sup>-</sup>, SbF<sub>6</sub><sup>-</sup> and BArF<sup>-</sup>; Fig. 4).<sup>46</sup> Complexes **10-X** (X = NO<sub>3</sub><sup>-</sup>, CF<sub>3</sub>COO<sup>-</sup>, CF<sub>3</sub>SO<sub>3</sub><sup>-</sup>, SbF<sub>6</sub><sup>-</sup>, BArF<sup>-</sup>) showed no activity. Complex **10-PF<sub>6</sub>** gave a 20% yield of the product while complex **10-BF<sub>4</sub>** gave 88% yield. These results are in strong contrast to previous results obtained using **5-BF<sub>4</sub>** and **5-BArF** as catalysts, where the counter ion showed no influence.<sup>33</sup> The reaction

mechanism of the catalysis with **10-BF<sub>4</sub>** was investigated by DFT/B3LYP computations. It was found that the formation of ethyl 3-hydroxy-2-arylacrylates had a lower energy barrier compared to the formation of the β-keto ester. Hydrogen bonds between the acidic N–H of the ligand, the BF<sub>4</sub><sup>-</sup> anion and the EDA (N–H...F–BF<sub>2</sub>–F...EDA) seemed to play an important role.<sup>46</sup>

## 2.2 Iron(II) PNP pincer complexes for catalytic hydrogenation

Chirik and co-workers reported that the dinitrogen *cis*-dihydride complex [(<sup>i</sup>PrP<sup>C</sup>N<sup>C</sup>P)Fe(H)<sub>2</sub>(N<sub>2</sub>)] (**11**, Fig. 6) catalyzed the hydrogenation of simple acyclic and cyclic alkenes.<sup>24</sup> The hydrogenation of 1-hexene under 4 bar of H<sub>2</sub> was achieved using a 0.3 mol% catalyst loading in three hours and with a conversion of more than 98%. The conversion for the hydrogenation of cyclohexene was only 10%. Milstein and co-workers developed a new iron pincer complex [(<sup>i</sup>PrP<sup>C</sup>N<sup>C</sup>P)FeH(CO)Br] (**12**, Fig. 6).<sup>26</sup> The complex was active for the hydrogenation of ketones under mild conditions. The reactions typically proceeded in an ethanolic solution with 0.05 mol% of **12** under 4 bar of hydrogen pressure and temperatures of 26–28 °C. A maximum TON of 1880 was reached. A wide range of aromatic and aliphatic ketones could be hydrogenated. The catalysis was less selective for enone substrates such as *E*-4-phenylbut-3-en-2-one and cyclohex-2-enone, where the C=C double bonds were preferably hydrogenated. Interestingly, for benzaldehyde only 36% of benzylic alcohol could be isolated after the hydrogenation. The low yield might be due to catalyst poisoning by benzoic acid, which was formed in small quantities *via* a Cannizzaro reaction. By lowering the catalyst loading to 0.025 mol%, increasing the loading of KO<sup>*t*</sup>Bu (base) to 0.625% and running the reaction in an ethanol/NEt<sub>3</sub> (2 : 1) solution at 40 °C under 30 bar H<sub>2</sub>, the yield for the hydrogenation of benzaldehyde could be increased to up to 99% and the TON was up to 4000. This modified protocol was applied for the hydrogenation of various aromatic and aliphatic aldehydes.<sup>31</sup>

For the hydrogenation of ketones catalyzed by **12**, the reactions were best run in ethanol; in THF or neat acetophenone no conversion was observed. Stoichiometric reactions revealed that the bridging methylene group of **12** was deprotonated by KO<sup>*t*</sup>Bu to form the complex [(<sup>i</sup>PrP<sup>C</sup>N<sup>C</sup>P<sup>H</sup>)FeH(CO)] (**13**, Fig. 7) containing a dearomatized pyridine ligand. It was proposed



**Fig. 4** Reaction of *p*-anisaldehyde with EDA catalyzed by **5-X** (X<sub>2</sub> = BF<sub>4</sub><sup>-</sup>, BArF<sup>-</sup>) and **10-X** (X = NO<sub>3</sub><sup>-</sup>, CF<sub>3</sub>COO<sup>-</sup>, CF<sub>3</sub>SO<sub>3</sub><sup>-</sup>, BF<sub>4</sub><sup>-</sup>, PF<sub>6</sub><sup>-</sup>, SbF<sub>6</sub><sup>-</sup> and BArF<sup>-</sup>).



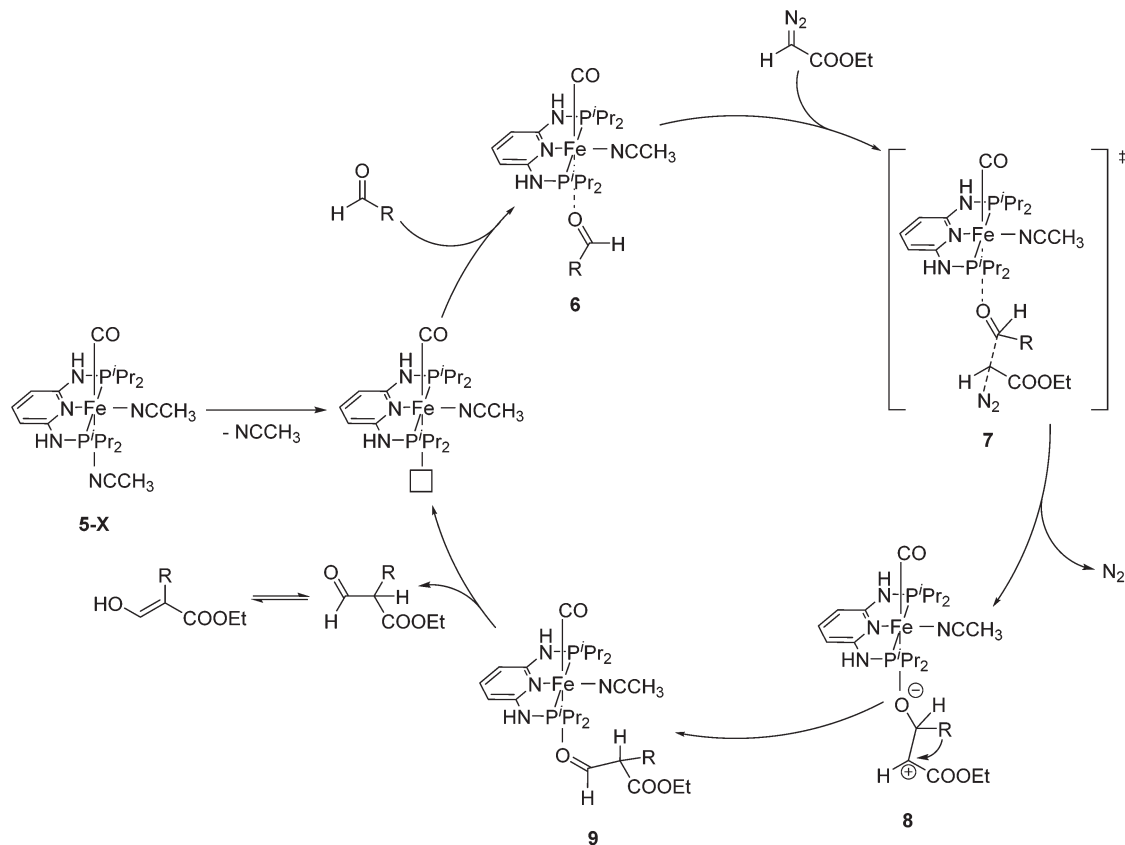


Fig. 5 Mechanistic proposal for the formation of ethyl 3-hydroxy-2-(4-methoxyphenyl)acrylate from *p*-anisaldehyde and EDA.



Fig. 6 Structures of complexes **11**, **12**, **17** and **18**.

that the 5-coordinated 16-electron species **13** might be stabilized by the reversible addition of ethanol to afford the 6-coordinate species **13'**. In the proposed mechanism, the coordination of ketone to **13** followed by insertion into the iron–hydride bond gave the alkoxide complex **14**. The coordination of dihydrogen to **14** then gave intermediate **15**. Heterolytic cleavage of the dihydrogen in **15** then generated either the hydrido alkoxide complex **16** or its dearomatized form **16'**. The catalytic cycle was closed by elimination of the alcohol and regeneration of **13**.<sup>26,47</sup>

The Milstein group further found that minor modifications of the  $[(iPrP^CN^CP)FeH(CO)Br]$  (**12**) catalyst led to base-free hydrogenation of ketones.<sup>28</sup> They found that  $[(iPrP^CN^CP)FeH(CO)(\eta^1BH_4)]$  (**17**, Fig. 6) catalyzed the hydrogenation of aceto-

phenone under 4 bar of hydrogen at 40 °C without the need for an additional base. Aromatic and aliphatic ketones could be readily reduced to the corresponding alcohols with yields of 53% to 99%. Interestingly, a related complex,  $[(iPrP^CN^CP)FeH(\eta^2BH_4)]$  (**18**, Fig. 6), was not active. In aprotic solvents such as benzene-*d*<sub>6</sub> and toluene-*d*<sub>8</sub>,  $[(iPrP^CN^CP)FeH(CO)(\eta^1BH_4)]$  (**17**) loses  $BH_3$  to give *trans*- $[(iPrP^CN^CP)Fe(H)_2(CO)]$ , which is in equilibrium with *cis*- $[(iPrP^CN^CP)Fe(H)_2(CO)]$ . Neither complex reacts with acetophenone, excluding its participation in the catalytic cycle.

Kirchner and co-workers recently synthesized a series of  $[(iPrP^NN^NP)FeH(CO)L]^n$  (**19-L**) complexes with  $L = Br, CH_3CN, pyridine, PMe_3, SCN^-, CO$  and  $BH_4^-$  and  $n = 0$  and  $+1$ .<sup>39</sup> The spacers between the phosphine and pyridine donors were NH



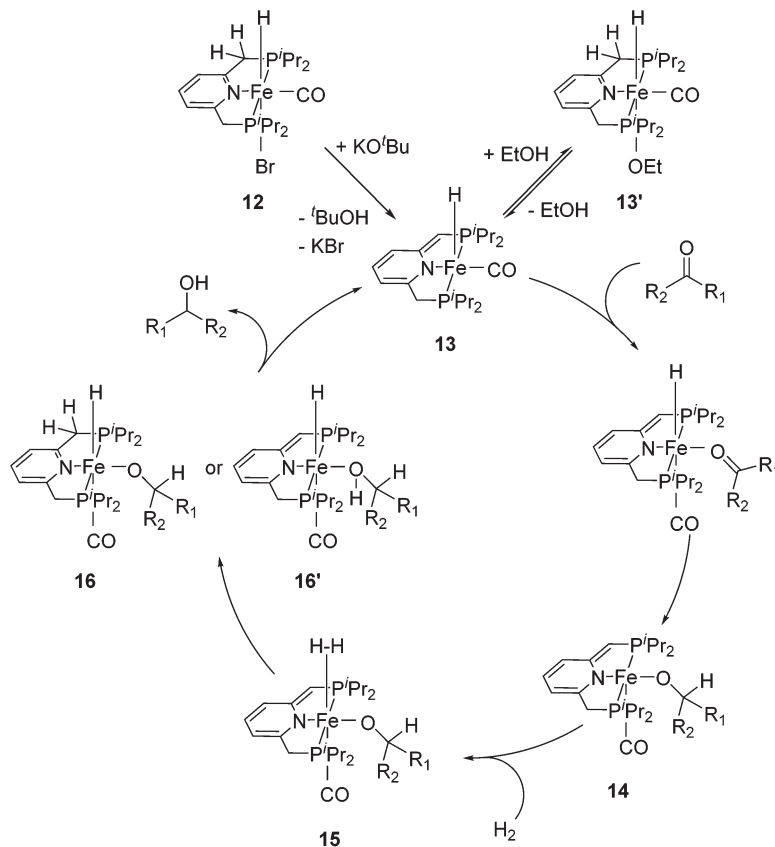


Fig. 7 Proposed catalytic cycle for the hydrogenation reactions of ketones using  $[(iPrPCNP)FeH(CO)Br]$  (**12**) as a pre-catalyst.

and/or NMe. Complex **19a-Br** (Fig. 8) was active in the hydrogenation of acetophenones under 5 bar hydrogen at 25 °C, with a catalyst loading of 1.0 mol% and 2.0 mol% KOtBu as the base. The hydrogenation only occurred in alcoholic solutions, with ethanol being the best solvent. Complex **19b-Br** was completely inactive while complex **19c-Br** had low activity. Changing the Br ligand of **19a-Br** to  $CH_3CN$  and  $BH_4^-$  resulted in similarly active catalysts. Changing the Br ligand to pyridine,  $PMe_3$ ,  $SCN^-$ , CO, however, led to inactive complexes, because these ligands probably could not dissociate during catalysis. The turnover frequency (TOF) was up to  $770\text{ h}^{-1}$ . Interestingly, both **19a-Br** and **19b-Br** were active for the hydrogenation of aldehydes. Thus, **19b-Br** is a chemoselective cata-

lyst for the hydrogenation of aldehydes. The mechanism of hydrogenation catalyzed by **19a-Br** was investigated by stoichiometric reactions and DFT computations.<sup>39</sup> The results suggested that **19a-Br** reacted with one equivalent of a base to afford the deprotonated 5-coordinated complex  $[(iPrP^N N^N P^H)FeH(CO)]$  (**20**; Fig. 9). An incoming ketone coordinated to the vacant coordination site on the complex and inserted into the iron-hydride bond to give the 5-coordinated alkoxide complex  $[(iPrP^N N^N P^H)Fe(OCHR_1R_2)(CO)]$  (**21**;  $OCHR_1R_2 = \text{alkoxide}$ ). Hydrogen then bound to **21** to give  $[(iPrP^N N^N P^H)Fe(H_2)(OCHR_1R_2)(CO)]$  (**22**). The heterolytic cleavage of hydrogen with the aid of the coordinated alkoxide led to the formation of an alcohol and regeneration of the hydride species  $[(iPrP^N N^N P^H)FeH(HOCHR_1R_2)(CO)]$  (**23**). Substitution of the alcohol by an incoming ketone closed the catalytic cycle. It was shown that the amine stays deprotonated throughout the catalytic cycle. The heterolytic cleavage of  $H_2$  involving protonation of the alkoxide ligand had a calculated barrier of  $16.0\text{ kcal mol}^{-1}$ , much lower than the  $34.1\text{ kcal mol}^{-1}$  calculated for the heterolytic cleavage involving the deprotonated PNP ligand. The role of ethanol seemed to prevent the formation of unactive Fe dihydride species.

Hu and co-workers recently synthesized  $[(iPrP^O N^O P)FeH(CO)L]^n$  (**24-L**;  $L = CH_3CN$  or Br and  $n = 0$  or  $+1$ ; Fig. 10) complexes, where  $L = CH_3CN$  or Br and  $n = 0$  or  $+1$ .<sup>41</sup> The phos-

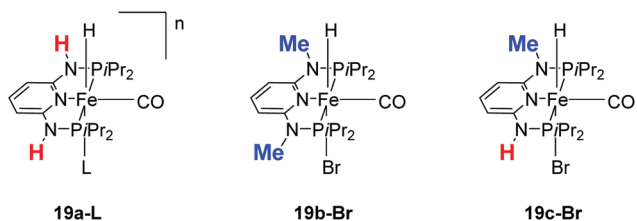


Fig. 8 Structures of complexes **19a-L** ( $L = Br, CH_3CN, py, PMe_3, SCN^-, CO$  and  $BH_4^-$ ;  $n = 0, +1$ ), **19b-Br** and **19c-Br**.





Fig. 9 Proposed catalytic cycle for the hydrogenation reactions of ketones using  $[(i^{\text{Pr}}\text{P}^{\text{N}}\text{N}^{\text{P}})\text{Fe}(\text{CO})\text{Br}]$  (**19a-Br**) as a pre-catalyst.



Fig. 10 Structure of  $[(i^{\text{Pr}}\text{P}^{\text{O}}\text{N}^{\text{O}}\text{P})\text{Fe}(\text{CO})\text{L}]^n$  (**24-L**;  $\text{L} = \text{CH}_3\text{CN}$  or  $\text{Br}$  and  $n = 0$  or  $+1$ ).

phinite donors are linked to the central pyridine ring by oxygen atoms, so a dearomatization of the central pyridine ring upon deprotonation of the linker, as shown in the complexes of Milstein and Kirchner<sup>26,27,31,39</sup> is not possible. Complex **24-Br** is a chemoselective catalyst for the hydrogenation of aldehydes. The scope of the reaction was probed for a range of different aliphatic and aromatic aldehydes, using 10 mol% of **24-Br** in methanol under 8 bar hydrogen at room temperature (Table 1). Importantly, functional groups such as terminal and internal alkenes,  $\alpha,\beta$ -unsaturated aldehydes and keto were tolerated. The addition of 10 mol%  $\text{HCOONa}$  promoted the reaction. The catalyst loading and the  $\text{H}_2$  pressure could be reduced to 5 mol% and 4 bar, respectively (Table 2). While **24-CH<sub>3</sub>CN** was not active for hydrogenation under the

Table 1 Hydrogenation aldehydes using 10 mol% **24-Br** as the catalyst

Entry	Aldehyde	Product	Yield <sup>a</sup> [%]
1			90 (82)
2			88 (65)
3			94 (90)
4			96 (85)
5			80 (74)
6			74
7			60
8			65 (60)
9			55

<sup>a</sup> Yield determined by GC (isolated yield).

conditions shown in Table 1, it was active when  $\text{HCOONa}$  was used as an additive.<sup>41</sup>

The promotion by  $\text{HCOONa}$  encouraged the study of **24-L** for transfer hydrogenation of aldehydes using sodium formate as the hydrogen donor. Indeed, both catalysts were active and chemoselective for this reaction (Table 2).<sup>41</sup>

Milstein and co-workers showed that *trans*- $[(^{\text{tBu}}\text{P}^{\text{C}}\text{N}^{\text{C}}\text{P})\text{Fe}(\text{H})_2\text{CO}]$  (**25**; Fig. 11) catalyzed the hydrogenation of sodium bicarbonate.<sup>27</sup> A TON of up to 788 and a TOF of up to  $156 \text{ h}^{-1}$  were obtained. The yields of sodium formate were around 40%. NMR and IR studies suggested that carbon dioxide inserted into one iron hydride bond to give  $[(^{\text{tBu}}\text{P}^{\text{C}}\text{N}^{\text{C}}\text{P})\text{Fe}(\text{H})(\eta^1\text{-OOCH})\text{CO}]$  (**26**). The structure of this compound was confirmed by X-ray analysis. The formate ligand in **26** was easily replaced by water to form  $[(^{\text{tBu}}\text{P}^{\text{C}}\text{N}^{\text{C}}\text{P})\text{Fe}(\text{H})(\text{H}_2\text{O})\text{CO}]$  (**27**). A catalytic cycle was proposed (Fig. 12), in which the coordination of hydrogen to **27** gives  $[(^{\text{tBu}}\text{P}^{\text{C}}\text{N}^{\text{C}}\text{P})\text{Fe}(\text{H})(\text{H}_2)\text{CO}]$  (**28**). An incoming hydroxide deprotonated the hydrogen *via* heterolytic cleavage (**29**). This might involve the deprotonation of the PNP ligand forming the dearomatized complex **29'**. Either way, after elimination of water the starting dihydride complex **25** was regenerated.<sup>27</sup> Complex **25** was also an active catalyst for the decomposition of formic acid, with a TON of up to 100 000.<sup>29</sup>



Table 2 Hydrogenation reaction with NaOOCH as a promoter (cond. A) and transfer hydrogenation (cond. B) of aldehydes

Entry	Aldehyde	Product	Yield <sup>a</sup> [%]		Yield <sup>a</sup> [%]	
			Cond. A		Cond. B	
			24-Br	24-CH <sub>3</sub> CN	24-Br	24-CH <sub>3</sub> CN
			cond. A: NaOOCH (10 mol%) 4 bar H <sub>2</sub> r.t., 24 h		cond. B: NaOOCH (5 equiv) 40°C, 6 h	
1			80 (75)	75	98 (91)	95
2			83 (80)	94	98 (93)	94
3			86 (81)	76	98 (91)	95
4			92 (88)	72	97 (92)	85
5			56 (50)	53	93 (89)	86
6			95 (87)	76	99 (92)	96
7			71	57	82	79
8			66 (62)	76	99 (93)	96
9			84 (76)	82	n/a <sup>b</sup>	n/a <sup>b</sup>
10			87 (83)	92	97 (87)	95
11			84	90	97	84
12			58	65	98	94
13			65 (60)	78	85 (76)	72
14			(64)	(67)	(72)	(68)
15			70 (63)	64	78 (65)	69
16			60	68	95	90
17			75	83	95	75

<sup>a</sup> Yield determined by GC (isolated yield). <sup>b</sup> Not accessible.







Fig. 11 Structure of *trans*-[(<sup>t</sup>BuP<sup>C</sup>N<sup>C</sup>P)Fe(H)<sub>2</sub>CO] (**25**).

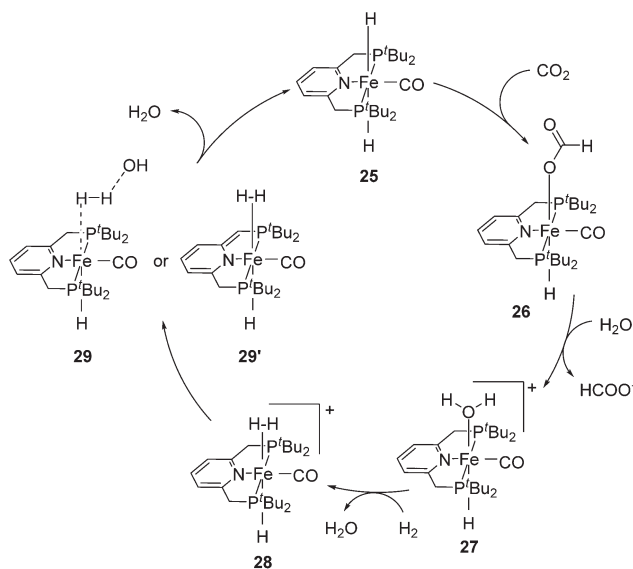


Fig. 12 Proposed mechanism for the hydrogenation of carbon dioxide catalyzed by *trans*-[(<sup>t</sup>BuP<sup>C</sup>N<sup>C</sup>P)Fe(H)<sub>2</sub>(CO)] (**25**).

### 3. Monoanionic benzene-based PCP ligand systems

The synthesis and application of PCP iron complexes are less reported than their PNP counterparts. These complexes are mostly formed *via* cyclometalation reactions. To promote the iron–carbon bond formation, iron precursors in a low oxidation state or with basic ligands such as alkoxides and alkyl groups are used.<sup>48–50</sup>

Creaser and Kaska reported the synthesis of [(<sup>Me</sup>P<sup>C</sup>C<sup>C</sup>P)Fe(H)(dmpe)] (**30**, Fig. 13).<sup>51</sup> Treating the <sup>Me</sup>P<sup>C</sup>C<sup>C</sup>P ligand with hydrated ferrous chloride in an ethanolic solution resulted in

the precipitation of a white polymeric compound [(<sup>Me</sup>P<sup>C</sup>C<sup>C</sup>P)FeCl<sub>2</sub>]<sub>n</sub> (**A**). This polymeric compound was converted to **30** in the presence of dmpe (1,2-bis(dimethylphosphino)ethane) and 30% sodium amalgam. The structure and composition of **30** were confirmed by NMR and IR. The insertion of a Fe ion into the C–H bond of benzene was proposed to take place when the Fe(II) ion was reduced to Fe(0).

Guan and co-workers synthesized [(<sup>R</sup>P<sup>O</sup>C<sup>O</sup>P)FeH(PMe<sub>3</sub>)<sub>2</sub>] (**31-R**; R = *i*Pr, Ph; Fig. 15)<sup>52,53</sup> by cyclometalation of the <sup>R</sup>P<sup>O</sup>C<sup>O</sup>P ligand with Fe(0)(PMe<sub>3</sub>)<sub>4</sub>. **31-*i*Pr** catalyzed the hydrosilylation of various aryl aldehydes by (EtO)<sub>3</sub>SiH. Aryl ketones were less reactive under similar reaction conditions. In order to gain some mechanistic insights, stoichiometric reactions were probed. Benzaldehyde did not react with **31-*i*Pr**, excluding its insertion into the Fe–H bond as a catalytic step. The reaction of **31-*i*Pr** with CO for 24 hours at room temperature gave quantitatively [(<sup>i</sup>PrP<sup>O</sup>C<sup>O</sup>P)FeH(PMe<sub>3</sub>)(CO)] (**32**), where the CO ligand was *trans* to the hydride. This result was expected because the hydride had a strong *trans*-effect, which made the *trans* PMe<sub>3</sub> more labile than the *cis* one. Complex **32** slowly isomerized to the thermodynamically more stable complex [(<sup>i</sup>PrP<sup>O</sup>C<sup>O</sup>P)FeH(PMe<sub>3</sub>)(CO)] (**32'**) where CO was *cis* to the hydride, but the reaction took more than 7 days at 60 °C. The reaction of deuterium-labelled C<sub>6</sub>H<sub>5</sub>CDO with a mixture of Ph<sub>2</sub>SiD<sub>2</sub> and **31-*i*Pr** (1 : 1 : 1) led to the formation of Ph<sub>2</sub>SiD(OCD<sub>2</sub>C<sub>6</sub>H<sub>5</sub>) and Ph<sub>2</sub>Si(OCD<sub>2</sub>C<sub>6</sub>H<sub>5</sub>)<sub>2</sub> in a ratio of 4 : 1. No deuterium incorporation in **31-*i*Pr** was detected. This result further excluded the involvement of the hydride in **31-*i*Pr** in the hydrosilylation reaction. Based on the above results Guan and co-workers proposed the following mechanism (Fig. 14).<sup>52</sup>

The PMe<sub>3</sub> in **31-*i*Pr** *trans* to the hydride dissociated to give a vacant coordination site (**33**, Fig. 14). The isomerisation in which the remaining PMe<sub>3</sub> ligand moved to a position *trans* to the hydride was too slow to be catalytically relevant. An incoming carbonyl compound might coordinate to the open site at first before being reduced by silane (**34**, Fig. 14; cycle I). Alternatively, silane might first coordinate to the vacant site, get activated, and then reduce the carbonyl compound (**35**, Fig. 14; cycle II).<sup>52</sup> The details of these steps were not clear. Wang *et al.* reported a DFT study on the mechanism of this hydrosilylation reaction, favouring cycle I. They found that the carbonyl-coordinated compound underwent an isomerization to move PMe<sub>3</sub> to a position *trans* to the hydride. This was followed by the insertion of the carbonyl compound into the Fe–H bond, giving an iron alkoxide complex. The cycle was



Fig. 13 Synthesis of [(<sup>Me</sup>P<sup>C</sup>C<sup>C</sup>P)Fe(H)(dmpe)] (**30**).





Fig. 14 Proposed mechanism for the hydrosilylation of carbonyl compounds catalyzed by **31-iPr**.

closed by  $\sigma$ -bond metathesis with silane, yielding silyl ether and regenerating the iron hydride species.<sup>54</sup> The computed mechanism, however, was at odds with the experimental findings, which excluded the insertion of benzaldehyde into the Fe-hydride of **31-iPr** as a relevant step.<sup>52</sup>

Guan and co-workers also used **31-iPr** for the decomposition of  $\text{NH}_3\text{BH}_3$  (AB) to give  $\text{H}_2$  (Fig. 15).<sup>55</sup> The reactivity of **31-iPr** could be increased by replacing the two  $\text{PMe}_3$  ligands with  $\text{PMe}_2\text{Ph}$ , giving the complex  $[(^i\text{PrP}^{\text{O}}\text{C}^{\text{O}}\text{P})\text{Fe}(\text{H})(\text{PMe}_2\text{Ph})_2]$  (**36**). Complex **36**, which showed an increased activity in the beginning of the reaction, was less stable than **31-iPr** during the reaction. A further attempt was undertaken to increase the electron density of the metal center, by adding a methoxy group *para* to the Fe-C bond (**37**, Fig. 15). Complex **37** was indeed more active than **31-iPr** and **36**, and more stable than **36**.<sup>55</sup>

Recently Guan and co-workers prepared cationic complexes  $[(^i\text{PrP}^{\text{O}}\text{C}^{\text{O}}\text{P})\text{Fe}(\text{PMe}_3)(\text{CO})](\text{BF}_4)$  (**38**) and *cis*- $[(^i\text{PrP}^{\text{O}}\text{C}^{\text{O}}\text{P})\text{Fe}(\text{CO})_2](\text{BF}_4)$  (**39**) by the hydride abstraction of  $[(^i\text{PrP}^{\text{O}}\text{C}^{\text{O}}\text{P})\text{FeH}(\text{PMe}_3)(\text{CO})]$  (**40**) and  $[(^i\text{PrP}^{\text{O}}\text{C}^{\text{O}}\text{P})\text{FeH}(\text{CO})_2]$  (**41**) using a Brønsted acid such as  $\text{HBF}_4 \cdot \text{Et}_2\text{O}$ .<sup>56</sup> **38** and **39** were able to activate hydrogen in the presence of Hünig's base to give back the neutral hydride complexes **40** and **41**, respectively. **38** and **39** were

active catalysts for the hydrosilylation of benzaldehyde and acetophenone, with increased activity over the corresponding neutral complexes, **40** and **41**.<sup>56</sup>

#### 4. Pyridine- and phenyl bis(oxazolinyl) pincer systems

Iron pyridine bis(oxazoline) (pybox) complexes (Fig. 16) have been widely used in catalytic reactions. In the majority of the cases, these complexes were formed *in situ* by combining iron salts and pybox ligands. The reactions studied included cyclizations,<sup>57–60</sup> additions,<sup>61–65</sup> the kinetic resolution of racemic sulfoxides,<sup>66</sup> and hydrosilylation of aromatic ketones.<sup>67</sup> The active species were unclear, so they were not further discussed.

The groups of Huang and Nomura employed pre-made  $[(\text{pybox-R})\text{FeCl}_2]$  **42-R** ( $\text{R} = \text{Me}_2, \text{Ph}_2, \text{iPr}(\text{S})$ ) complexes as catalysts for the polymerisation of ethylene.<sup>68–70</sup> Redlich and Hossain prepared a series of  $[(\text{pybox-R})\text{FeCl}_2]$  (**42-R**;  $\text{R} = \text{iPr}(\text{S}), \text{tBu}(\text{S}), \text{Ph}(\text{S})$ ) complexes and used them for the cyclopropanation of imines (Fig. 17).<sup>45</sup> In the presence of one equivalent of



Fig. 15 Activity of Fe-POCOP complexes **31-iPr**, **36** and **37** for the decomposition of amine borane.





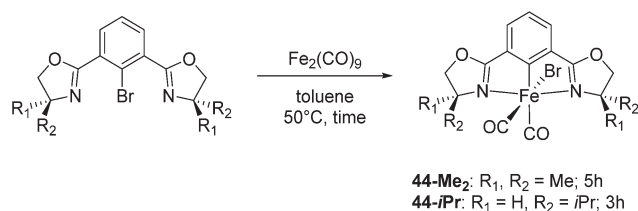
**Fig. 16** Structures of complexes **42-R** (R = Me<sub>2</sub>, Ph<sub>2</sub>, *i*Pr(S), *t*Bu(S), Ph(S)) and **43-R** (R = *i*Pr(S), *t*Bu(S), Bn(S), *i*Bu(S)).



**Fig. 17** Cyclopropanation catalyzed by complexes **42-R** (R = *i*Pr(S), *t*Bu(S)).

the halide abstractor, AgSbF<sub>6</sub> (relative to catalyst), **42-R** (R = *i*Pr, *t*Bu) catalyzed the reaction to yield 47% of the *cis*-aziridine with ee's below 50%. The *trans*-aziridine and β-amino-α,β-unsaturated esters were side products.

Chirik and co-workers studied enantioselective hydrosilylation of ketones using chiral iron pybox complexes<sup>71</sup> [(pybox-R)Fe(CH<sub>2</sub>SiMe<sub>3</sub>)<sub>2</sub>] (**43-R**; R = *i*Pr(S), *t*Bu(S), indane(1*R*,2*S*), Bn(S), *i*Bu(S); Fig. 16). The results in Table 3 show that the catalysts were generally active, and the reactions have high yields and a broad functional group tolerance. Bulky substrates (2,4,6-trimethylacetophenone and 2,6-dimethyl-4-*t*Bu-acetophenone), however, could not react. The enantioselectivity was low in all cases. Nishiyama and co-workers synthesized iron complexes of a phenyl-bis(oxazoline) (phebox) ligand (**44-R**, Fig. 18). The synthesis involved the reaction of Fe<sub>2</sub>(CO)<sub>9</sub> with (phebox-R)Br (R = Me<sub>2</sub>, *i*Pr(S)), probably *via* oxidative addition of the C-Br bond at the Fe center (Fig. 18).<sup>72</sup>



**Fig. 18** Reaction scheme for the complexation of [(phebox-R)FeBr(CO)<sub>2</sub>] (**44-R**; R = Me<sub>2</sub>, *i*Pr(S)).

**Table 3** Hydrosilylation of ketones catalyzed by complex **43-R** (R = *i*Pr(S), *t*Bu(S), indane(1*R*,2*S*), Bn(S), *i*Bu(S))<sup>a</sup>

Entry	Compound	R = <i>i</i> Pr(S)	<i>i</i> Pr(S) <sup>b</sup>	<i>t</i> Bu(S)	Bn(S)	<i>i</i> Bu(S)
1		80 (49)	99 (54)	99 (30)	99 (18)	99 (8)
2	R = H					
3	R = 4- <i>t</i> Bu	99 (23)	99 (13)	99 (25)	99 (25)	99 (11)
4	R = 4-OMe	99 (5)	55 (25)	99 (3)	99 (29)	97 (5)
5	R = 4-CF <sub>3</sub>	99 (20)	99 (20)	99 (12)	99 (21)	99 (12)
6	R = 3,5-(CF <sub>3</sub> ) <sub>2</sub>	99 (6)	99 (6)	72 (12)	99 (6)	99 (4)
7	R = 2,4-(OMe) <sub>2</sub>	99 (32)	99 (32)	99 (50)	99 (32)	99 (22)
8	R = 2,4,6-Me <sub>3</sub>	<1	1 (30)	2 (5)	4 (44)	2 (26)
9	R = 2,6-Me <sub>2</sub> -4- <i>t</i> Bu	<1	<1	1 (30)	<1	<1
10		99 (30)	99 (41)	60 (2)	93 (22)	25 (7)
11		58 (10)	99 (11)	99 (25)	46 (17)	46 (17)

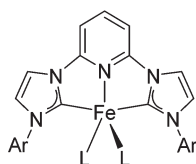
<sup>a</sup> Conversion [%] (ee [%]). <sup>b</sup> The catalyst was activated by the addition of 0.95 equivalents of B(C<sub>6</sub>F<sub>5</sub>)<sub>3</sub>.



The chiral complex **44-iPr(S)** catalyzed hydrosilylation of aromatic ketones. The reduction of 4-acetylbiphenyl in the presence of 2 mol% **44-iPr(S)** and 2 mol% of Na(acac) in hexane at 50 °C gave 1-(4-biphenyl)ethanol in a 99% yield and 66% ee for the *R*-configuration. The reduction of 2-acetylanthracene and 2-acetylnaphthalene gave 49 and 53% ee, respectively. However, the reduction of 1-acetyl-4-methoxybenzene and 1-acetyl-4-methylbenzene had low enantioselectivity (21–38%).<sup>72</sup>

## 5. Pyridine bis(*N*-heterocyclic carbene) pincer systems

Bedford and co-workers showed that the iron(II) pyridyl bis(carbene) pincer complex, **45-Br<sub>2</sub>** (Fig. 19) was an excellent catalyst for the cross coupling of alkyl halides with *p*-tolyl Grignard reagents (Table 4).<sup>73</sup> While chlorocyclohexane (Table 4, entry 1) was unreactive, bromocyclohexane and 4-bromo-1-methylcyclohexane could be coupled in 94 and 89%



**45-L<sub>2</sub>**: Ar = 2,6-*i*Pr<sub>2</sub>-C<sub>6</sub>H<sub>3</sub>; L = Br, N<sub>2</sub>  
**46-L<sub>2</sub>**: Ar = 2,6-Me<sub>2</sub>-C<sub>6</sub>H<sub>3</sub>; L = N<sub>2</sub>  
**47-L<sub>2</sub>**: Ar = 2,4,6-Me<sub>3</sub>-C<sub>6</sub>H<sub>2</sub>; L = N<sub>2</sub>

Fig. 19 Structures of **45-L<sub>2</sub>** (L = Br, N<sub>2</sub>), **46-(N<sub>2</sub>)<sub>2</sub>** and **47-(N<sub>2</sub>)<sub>2</sub>**.

Table 4 Coupling of 4-tolylmagnesium bromide with alkyl halides catalyzed by iron pyridyl bis(carbene) complex **45-Br<sub>2</sub>**

Entry	Substrate	Product	Yield [%]
1			94
2	X = Br		—
3	X = Cl		
4			89 <sup>a</sup>
4			71

<sup>a</sup> *trans* : *cis* = 69 : 31.

Table 5 Catalytic hydrogenation of tri and tetra substituted alkenes CNC (carbene) iron(0) dinitrogen complexes **45-(N<sub>2</sub>)<sub>2</sub>**–**47-(N<sub>2</sub>)<sub>2</sub>**

Entry	Compound	<b>45-(N<sub>2</sub>)<sub>2</sub></b>	<b>46-(N<sub>2</sub>)<sub>2</sub></b>	<b>47-(N<sub>2</sub>)<sub>2</sub></b>
1		>95 (1 h)	35 (1 h)	35 (1 h)
2		89 (12 h)	>95 (1 h)	>95 (1 h)
3		>95 (15 h)	>95 (1 h)	>95 (1 h)
4		20 (24 h)	>95 (12 h)	>95 (1 h)
5		4 (48 h)	68 (48 h) <sup>a</sup>	60 (48 h) <sup>a</sup>
6		0 (24 h)	0 (24 h)	0 (24 h)

<sup>a</sup> *cis* : *trans* = 3 : 1.

yields (Table 4, entries 2 and 3). 1-Bromooctane was coupled in a 71% yield.<sup>73</sup>

Chirik and co-workers synthesized the iron(0) complex **45-(N<sub>2</sub>)<sub>2</sub>** (Fig. 19) and employed it for the hydrogenation of ethyl 3-methyl-2-butenoate. A complete conversion was obtained after 1 hour.<sup>74</sup> The results prompted the examination of analogous complexes bearing sterically less demanding aryl substituents, **46-(N<sub>2</sub>)<sub>2</sub>** and **47-(N<sub>2</sub>)<sub>2</sub>** (Fig. 19).

Table 5 compares the activity of complexes **45-(N<sub>2</sub>)<sub>2</sub>**–**47-(N<sub>2</sub>)<sub>2</sub>** in the hydrogenation of various internal alkenes (5 mol% catalyst, 4 atm H<sub>2</sub>, room temperature). The hydrogenation of ethyl 3-methyl-2-butenoate using **46-(N<sub>2</sub>)<sub>2</sub>** or **47-(N<sub>2</sub>)<sub>2</sub>** as a catalyst was less efficient as compared to that using **45-(N<sub>2</sub>)<sub>2</sub>** as a catalyst, due to competing deactivation pathways.<sup>75</sup> However, for other acyclic trisubstituted olefins, **46-(N<sub>2</sub>)<sub>2</sub>** and **47-(N<sub>2</sub>)<sub>2</sub>** are as active as **45-(N<sub>2</sub>)<sub>2</sub>**. They are even more active for the hydrogenation of cyclic trisubstituted olefins. A cyclic tetrasubstituted olefin could be hydrogenated using **46-(N<sub>2</sub>)<sub>2</sub>** or **47-(N<sub>2</sub>)<sub>2</sub>**, but acyclic tetrasubstituted olefins could not be hydrogenated.<sup>74</sup>

## 6. *N,N*-Diphenylamino-based pincer systems

Milstein and co-workers prepared iron complexes of an acridine ligand [(<sup>Ac</sup>PNP)FeBr<sub>2</sub>] (**48**) and [(<sup>HAc</sup>PNP)Fe(CH<sub>3</sub>CN)(μ<sup>2</sup>-CH<sub>3</sub>CHNBH<sub>3</sub>)] (**49**) (Fig. 20, <sup>Ac</sup>PNP = 4,5-bis(diphenylphosphino)acridine, <sup>HAc</sup>PNP = 4,5-bis(diphenylphosphino)-9*H*-acridine-10-ide).<sup>76</sup> Interestingly, in complex **49** the acridine is in





Fig. 20 Synthesis of **48** and **49**.

Table 6 Hydrogenation of internal alkynes catalyzed by **49**

$$R_1-C\equiv C-R_2 \xrightarrow[H_2, THF]{\mathbf{49}} R_1-CH=CH-R_2 + R_1-CH_2-CH_2-R_2$$

Entry	Alkyne	<b>49</b> [mol%]	Time [h]	Pressure [bar]	Yield [%]	<i>E</i> : <i>Z</i>
1		0.6	12	4	99	100 : 0
2	R = H	0.6	36	4	99	99 : 1
3	R = OMe	2	65	4	99	64 : 36
4	R = COCH <sub>3</sub>	2.2	22	4	89 (11) <sup>a</sup>	99 : 1
5	R = COOEt	4	72	10	94	99 : 1
6	R = CN	2.2	23	10	87 (13) <sup>a</sup>	99 : 1
7	R = Cl	2.5	70	10	99	99 : 1
8		4	21	4	98 (2) <sup>a</sup>	100 : 0
9		2	48	4	70 (30) <sup>a</sup>	61 : 39
10		1.7	17	4	76 (24) <sup>a</sup>	99 : 1
11		1	30	4	85	100 : 0
12		0.6	11	4	99	—

<sup>a</sup> The yield in parentheses is the corresponding alkane product [%].

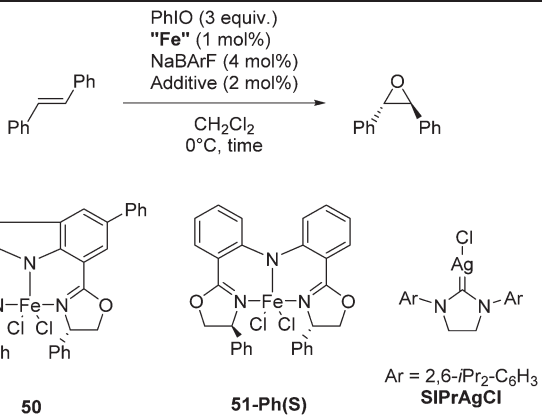
the reduced form and the  $\mu^2$ -CH<sub>3</sub>CHNBH<sub>3</sub> ligand originates from the insertion of acetonitrile into BH<sub>4</sub><sup>-</sup>.

**48** and **49** were employed for hydrosilylation of internal alkynes. While **48** was not active, **49** was an efficient and selective catalyst (Table 6). The yields were generally between 85 to 100%, and the reactions were *E*-selective. A high functional

group tolerance was obtained: ether, ester, ketone, halide and nitrile substituents remained intact during the reduction. A terminal alkyne, phenylacetylene, could also be reduced.<sup>76</sup>

Niwa and Nakada developed a carbazole-based tridentate bis(oxazoline) ligand (CarBox-R) that displayed porphyrin-like properties in the iron catalyzed epoxidation reaction of



**Table 7** Asymmetric epoxidation of *trans*-stilbene using **50** and **51** as catalysts


Entry	Complex	Additive	Time [min]	Yield [%]	ee [%]
1	<b>50</b>	None	30	35	83
2	<b>50</b>	None	60	Trace	n/a
3	<b>50</b>	SIPrAgCl	60	55	88
4	<b>51</b>	SIPrAgCl	60	Trace	n/a

(*E*)-olefins.<sup>77</sup> In the presence of 4 mol% NaBARf, [(CarBox-Ph)-FeCl<sub>2</sub>] (**50**, 1 mol%) catalyzed the epoxidation of *trans*-stilbene using iodobenzene as an oxidising reagent (Table 7). The reaction gave a 35% yield with an ee of 83%. In the absence of NaBARf no reaction was observed. When SIPrAgCl (SIPr = *N,N'*-bis(2,6-*i*Pr<sub>2</sub>-C<sub>6</sub>H<sub>3</sub>)-4,5-dihydroimidazol-2-ylidene) was used as an additive the yield and ee could be increased to 55% and 88%, respectively. The reaction with the structurally similar [(bopa-Ph)FeCl<sub>2</sub>] (**51-Ph(S)**; *vide infra*) gave no yield. The investigation of the substrate scope showed the broad utility of this reaction. Various substituted *trans*-stilbenes and cinnamyl alcohol derivatives reacted to give the corresponding (*S,S*) epoxides in high enantioselectivity.<sup>77</sup>

Nishiyama and co-workers studied the enantioselective hydrosilylation of ketones catalyzed by iron bis(oxazolinylphenyl)amino complexes (bopa-R; **53-R(S)**; R = dpm (CH(Ph)<sub>2</sub>), *i*Pr, *t*Bu, Ph, Bn). The reduction of 4-acetylbiphenyl by (EtO)<sub>2</sub>MeSiH was used as test reaction. The best results were obtained with **53-dpm(S)**, with a 99% yield and a 72% ee (Fig. 21). The scope of the reaction was then further probed (Table 8; condition A). The yields were usually high and a range of functional groups were tolerated. The enantioselectivities were modest to good. The *R*-enantiomer was the major product.<sup>78</sup> Attempts to isolate the active complex by mixing iron(II) acetate with **53-R(S)** were unsuccessful. However, they were able to isolate [(bopa-*i*Pr)-Fe<sup>III</sup>Cl<sub>2</sub>] (**51-*i*Pr(S)**) from a refluxing mixture of FeCl<sub>2</sub> and **53-*i*Pr(S)** in THF under air. Interestingly, **51-*i*Pr(S)** was inactive for the hydrosilylation of 4-acetylbiphenyl under the previously described conditions.

In a subsequent study, Nishiyama and co-workers showed that **51-R** could be activated by the addition of 6 mol% Zn. The model substrate, 4-acetylbiphenyl, could be reduced in a 98% yield with a 65% ee.<sup>79</sup> But in this reaction the *S*-enantiomer was the major product, which is opposite to the reaction using the mixture of Fe(OAc)<sub>2</sub> with a ligand. The origin of the change in selectivity was unclear. The new reaction conditions were also general for the enantioselective hydrosilylation of ketones (Table 8; condition B).

Hu and co-workers recently reported that complex **51-R** (R = *t*Bu(S), Ph(R)) was an excellent catalyst for the Kumada cross coupling reaction of non-activated alkyl halides (Table 9).<sup>80,81</sup> The protocol tolerates a range of functional groups, including carbamates (entry 11), N-heterocycles (entries 2 and 4), Boc-protected piperidine (entry 10), tetrahydropyran (entries 7 and 8), base-sensitive ester (entries 3 and 9) and ketone (entry 4). Natural product-derived compounds, including 3-iodocholestone, cholesteryl-6-iodohexanoate and menthyl-6-iodohexanoate (Table 9, entries 12–14) were also coupled in moderate to good yields. The enantioselectivity for the coupling of 3-iodobutylbenzene, 2-iodobutylbenzene and 2-iodopropylbenzene, however, was low. Only an ee of up to 20% could be obtained.<sup>80</sup>

**Fig. 21** Enantioselective hydrosilylation using the *in situ* formed iron catalyst.

**Table 8** The influence of Zn metal on the stereoselectivity in the hydrosilylation reaction of ketones

Entry	Ketone	Condition A			Condition B		
		Yield <sup>a</sup> [%]	ee [%]	Abs. config	Yield <sup>a</sup> [%]	ee [%]	Abs. config
					Condition A: Fe(OAc) <sub>2</sub> (5 mol%) <b>53-dpm(S)</b> (6 mol%) 24 h	Condition B: <b>51-dpm(S)</b> (5 mol%) Zn (6 mol%) 48 h	
1		98	78	R	99	63	S
2		99	54	R	99	76	S
3		95	50	R	99	36	S
4		99	40	R	99	55	S
5		99	71	R	99	82	S
6		99	85	R	99	80	S
7		97	90	R	99	95	S
8		93	86	R	99	81	S
9		97 <sup>c</sup>	89	R	99 <sup>b</sup>	95	S
10		94	35	S	99	33	S
11		88	58	R	98	1	S
12		57	15	R	87	60	S
13		40 <sup>b</sup>	18	S	40 <sup>b</sup>	32	S

<sup>a</sup> All reported yields were of the isolated product. <sup>b</sup> Reaction time was 96 hours. <sup>c</sup> Reaction time was 48 hours.



**Table 9** Cross coupling of alkyl halides with the phenyl Grignard reagent catalyzed by complex **51-tBu(S)**

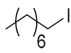
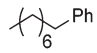
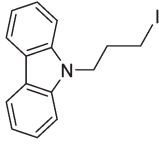
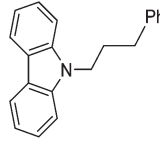
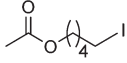
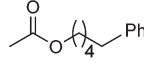
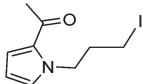
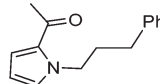
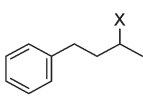
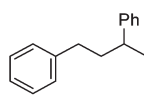
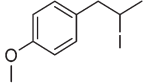
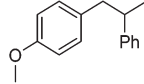
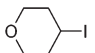
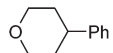
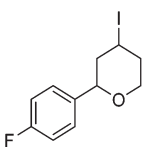
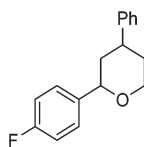
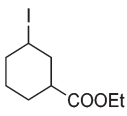
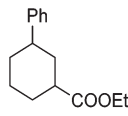
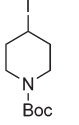
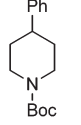
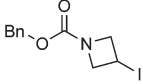
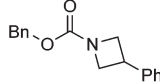
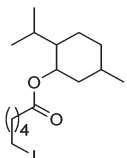
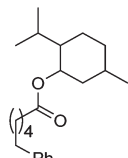
Entry	Halide	Product	Yield <sup>a</sup> (%)
$\text{R-X} + \text{PhMgCl} \xrightarrow[\text{THF, r.t., 1h}]{\text{51-tBu(S) (5 mol\%)}} \text{R-Ph}$ <p>R = Alkyl (1.0 equiv) X = Br, I</p>			
1			92 <sup>b,c</sup> 82 <sup>c</sup>
2			83
3			83
4			57 (25) <sup>d</sup>
5			95 <sup>b,c</sup> (X = I) 88 <sup>c</sup> (X = I) 93 <sup>c</sup> (X = Br)
6			90
7			75
8			92 <sup>e</sup>
9			71 <sup>f</sup>
10			88
11			65
12			83





Table 9 (Contd.)

		$\text{R-X} + \text{PhMgCl} \xrightarrow[\text{THF, r.t., 1h}]{\text{51-}t\text{Bu(S)} (5 \text{ mol}\%)} \text{R-Ph}$	
		R = Alkyl	(1.0 equiv)
		X = Br, I	
Entry	Halide	Product	Yield <sup>a</sup> (%)
13			53 <sup>g</sup>
14			85

<sup>a</sup> Isolated yields at 100% conversion. <sup>b</sup> Reaction at  $-40\text{ }^{\circ}\text{C}$ . <sup>c</sup> Use of **51-Ph(R)** as a catalyst. <sup>d</sup> 25% starting material was recovered. <sup>e</sup> Mixture of diastereoisomers: 66 : 34 (d.r. for RX = 91 : 9). <sup>f</sup> Mixture of diastereoisomers: 52 : 48 (d.r. for RX = 81 : 19). <sup>g</sup> Mixture of stereoisomers: 81 : 19 (d.r. for RX = 100 : 0).

## 7. 2,5-Disubstituted pyrrolidine-based pincer ligands

The group of Gade developed a new class of pincer ligands based on bis(oxazolinylmethylidene)isoindolines (boxmi).

Complex  $[(\text{boxmi-Ph(S)})\text{FeCl}(\text{S}_n)]$  (**54-Ph(S)**; S = solvent;  $n = 1$  or 2) was an active catalyst for the azidation of cyclic  $\beta$ -keto esters and 1-indanones (Table 10).<sup>82</sup> The indanone derived *tert* butyl  $\beta$ -keto esters could be converted in high yields and high enantioselectivities (90–93%) were achieved for many substrates. It was shown that the bulky *tert* butyl substituent on the ester is crucial for higher enantioselectivities (compare entry 7 with entry 9). Substituted cyclopentenone derivatives could also be converted in high enantioselectivity.<sup>82</sup>

Gade and co-workers then applied this catalytic system for the azidation of 3-aryloxindoles. The previously optimized conditions gave lower ee's. The selectivity could be increased by the *in situ* formation of the catalytically active species, which was generated by mixing 10 mol%  $\text{Fe}(\text{OOCt})_2$  with 12 mol% **55-Ph(S)** in diethylether at room temperature. Under the optimized reaction conditions the reactions of various 3-aryloxindoles were successful. The yields were between 85 and 90% and the ee were between 87 and 94% (Table 11).<sup>82</sup>

Gade and co-workers then showed that  $[(\text{boxmi-Ph(R)})\text{Fe}(\text{OAc})]$  (**56-Ph(R)**) and  $[(\text{boxmi-Ph(R)})\text{Fe}(\text{S})(\text{O-CH}_2\text{CH}_3\text{Ph})]$  (**57-Ph(R)**) catalyzed the enantioselective hydrosilylation of aryl ketones (Fig. 22).<sup>83</sup> The latter complex was employed for the hydrosilylation of various substrates (Table 12).

Good yields and selectivity were achieved for many substituted acetophenones. Different substituents had almost no influence on the outcome of the reaction. Changing the alkyl substituent of acetophenone to a more sterically demanding isopropyl group decreased the ee to 73% (entry 8). The use of diaryl ketones decreased the selectivity (entries 15 and 16). An inner sphere mechanism was proposed. Activation of the pre-catalyst gave an iron alkoxy complex, which undergoes  $\sigma$ -bond metathesis with silane to give the silyl ether product and the iron hydride species. The prochiral ketone coordinates to the hydride complex and subsequently inserts into the metal hydride bond to regenerate the iron alkoxy complex.<sup>83</sup>

## 8. Bis(phosphinoethyl)amino pincer ligands

Although pincer ligands were mostly based on rigid backbones such as arene, pyridine, and diarylamine, ligands based on more flexible alkyl linkers have also been reported. The  $\text{P}^{(\text{CH}_2)_2}\text{NH}^{(\text{CH}_2)_2}\text{P}$  ligand, also known as MACHO,<sup>84</sup> enforces a meridional coordination geometry on many transition metal ions. Their iron complexes have found many catalytic applications.<sup>3,85–95</sup>

Schneider and co-workers synthesized a series of different Fe(II) and Fe(0) complexes supported by  $\text{R}^{\text{P}^{(\text{CH}_2)_2}\text{NH}^{(\text{CH}_2)_2}\text{P}}$  (R = cy ( $\text{C}_6\text{H}_{11}$ ), iPr; Fig. 23).<sup>85</sup> The complexes  $[\text{Fe}(\text{R}^{\text{P}^{(\text{CH}_2)_2}\text{NH}^{(\text{CH}_2)_2}\text{P})-\text{Cl}_2(\text{CO})]$  (**58-R**; R = cy, iPr) were prepared by treating the ligand



**Table 10** Enantioselective azidation of cyclic  $\beta$ -keto esters catalyzed by complex **54-Ph(S)**

Entry	Product	Yield <sup>a</sup> [%]	ee [%]	Entry	Product	Yield <sup>a</sup> [%]	ee [%]
1		89	93 <sup>b</sup>	8		84	81
2		87	93	9		90	70
3		87	90	10		84	88
4		89	91	11		89	92
5		90	92	12		87	69
6		85	93	13		87	67 <sup>b</sup>
7		88	90	14		88	76

<sup>a</sup> All reported yields were of the isolated product. <sup>b</sup> Product was confirmed by the literature as *R*-enantiomer.

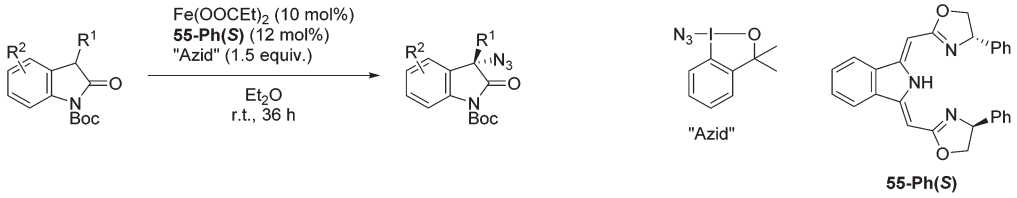
with  $\text{FeCl}_2$  under a CO atmosphere. Both **58-cy** and **58-iPr** show a low spin configuration. The Fe(0) complexes,  $[\text{Fe}(\text{R}^{\text{P}(\text{CH}_2)_2\text{NH}(\text{CH}_2)_2\text{P}}(\text{CO})_2)]$  (**59-R**; R = cy, iPr) were prepared by mixing  $\text{Fe}(\text{CO})_5$  with the ligand under UV irradiation. Both **59-cy** and **59-iPr** are in a low spin configuration. **59-R** reacted with  $\text{CH}_2\text{Cl}_2$  to give **58-R**. **59-iPr** reacted with HCl to give the cationic hydride species,  $[\text{Fe}(\text{iPrP}(\text{CH}_2)_2\text{NH}(\text{CH}_2)_2\text{P})\text{H}(\text{CO})_2]\text{Cl}$  (**60-iPr**). NMR spectroscopy suggested that both *cis* and *trans* CO isomers were formed. The neutral hydride complexes  $[\text{Fe}(\text{R}^{\text{P}(\text{CH}_2)_2\text{NH}(\text{CH}_2)_2\text{P}})\text{H}(\text{CO})\text{Cl}]$  (**61-R**) were obtained either by the reaction of **58-R** with  $\text{tBu}_4\text{NBH}_4$  in acetonitrile at room temperature or by UV irradiation of the cationic complex **60-R**. The reaction of **58-iPr** with an excess amount of  $\text{NaBH}_4$  (10 equiv.) generated the borohydride complex  $[\text{Fe}(\text{iPrP}(\text{CH}_2)_2\text{NH}(\text{CH}_2)_2\text{P})\text{H}(\text{CO})-$

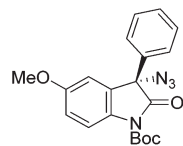
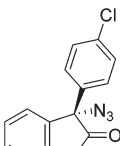
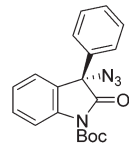
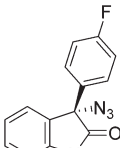
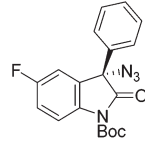
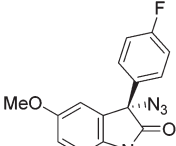
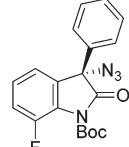
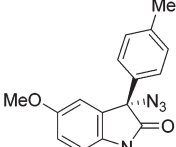
$(\eta_1\text{-HBH}_3)]$  (**62-iPr**). High resolution X-ray crystallography and NOESY experiments of **62-iPr** revealed an intramolecular hydrogen bond between the terminal hydrides of the  $\eta_1\text{-HBH}_3$  and the N-H of the ligand. Protonation of **62-iPr** with 2,6-lutidinium tetraphenylborate gave the dimeric complex  $[(\text{Fe}(\text{iPrP}(\text{CH}_2)_2\text{NH}(\text{CH}_2)_2\text{P})-\text{CO})_2(\mu_2, \eta_1:\eta_1\text{-H}_2\text{BH}_2)](\text{BPh}_4)$  (**63-iPr**). This compound is a group 8 metal complex with a  $\mu_2, \eta_1:\eta_1\text{-H}_2\text{BH}_2$  ligand.<sup>85</sup>

### 8.1 Hydrogenation of esters and nitriles

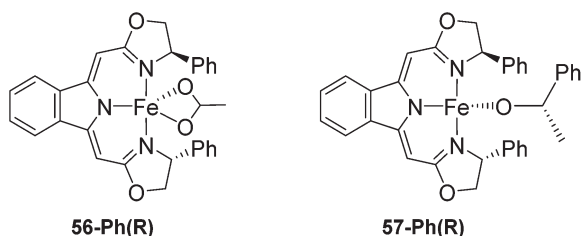
The groups of Guan and Beller independently reported the hydrogenation of esters to alcohols catalyzed by **62-iPr**.<sup>53,86,87</sup> Both aliphatic and aromatic esters were hydrogenated in moderate to high yields. Aromatic esters showed higher reactivity compared to the aliphatic esters. For a substrate containing



**Table 11** Enantioselective azidation of 3-aryloxoindolines catalyzed by an *in situ* formed iron catalyst


Entry	Product	Yield <sup>a</sup> [%]	ee <sup>b</sup> [%]	Entry	Product	Yield <sup>a</sup> [%]	ee <sup>b</sup> [%]
1		87	91	5		85	94
2		85	91	6		89	90
3		90	91	7		85	91
4		85	94	8		89	87

<sup>a</sup> All reported yields were of the isolated products. <sup>b</sup> The absolute configuration was determined by a crystal structure of an 1,2,3-triazole which was obtained by click reaction of the azide compound, entry 3 with (3-bromophenyl)acetylene. The configuration was confirmed as the *R*-enantiomer.

**Fig. 22** Structures of complexes [(boxmi-Ph(R))Fe(OAc)] (**56-Ph(R)**) and [(boxmi-Ph(R))Fe((S)-OCH<sub>2</sub>CH<sub>2</sub>Ph)] (**57-Ph(R)**).

both C=C and C=O groups, methyl cinnamate, hydrogenation of both groups was obtained.

Guan and co-workers then reported the hydrogenation of CE-1270, a methyl ester derived from coconut oil.<sup>86</sup> The substrate consisted of methyl laurate (C12, 73%), methyl myristate

(C14, 26%) and trace amounts of C10 and C16 methyl esters (~1%). The hydrogenation was carried out under neat conditions under 52 bar hydrogen pressure at 135 °C, using 1 mol% **62-iPr** as the catalyst. The reaction gave a full conversion after three hours, giving a combined GC yield of 99% for fatty alcohols. In an upscale experiment (100 g), the yield was only 25%, suggesting catalyst degradation. Lowering the temperature to 115 °C increased the yield to 40%.<sup>86</sup> Complex **62-iPr** was then further employed in the hydrogenation of neat coconut oil, without transforming it to the corresponding fatty acid methyl esters. A yield of 12% was reached after 23 hours.<sup>92</sup>

Beller and co-workers reported the hydrogenation of nitriles and dinitriles using **62-iPr** as the catalyst.<sup>91</sup> The catalyst showed good chemoselectivity, tolerating various functional groups (Table 13).



**Table 12** Enantioselective hydrosilylation of aromatic ketones catalyzed by **57-Ph(R)**

Entry	Product	ee [%]	Entry	Product	ee [%]
1		99	9		94
2		98	10		95
3		93	11		99
4		99	12		94 <sup>b</sup>
5		99	13		99
6		99	14		99
7		99	15		81
8		73 <sup>a</sup>	16		31

<sup>a</sup> 56% yield. <sup>b</sup> 4 equiv. of (EtO)<sub>2</sub>MeSiH were added.

Aryl nitriles with electron-donating groups could be reduced at a lower temperature than aryl nitriles with electron-withdrawing groups. The method could be employed for the hydrogenation of more challenging aliphatic nitriles.

## 8.2 Acceptorless dehydrogenation of alcohols, formic acid and N-heterocycles

Beller and co-workers showed that **62-iPr** and  $[\text{Fe}(\text{iPrP}(\text{CH}_2)_2\text{NH}(\text{CH}_2)_2\text{P})\text{H}(\text{CO})\text{Br}]$  (**64-iPr**; Fig. 24), were active catalysts for the dehydrogenation of methanol to give hydrogen and CO<sub>2</sub> in the presence of a base (8 M KOH) at 91 °C. The TON was up to 10 000 after 46 hours. In order to improve the stability of **62-iPr** in the reaction, an additional ligand (up to 5 equivalents) was added. The life time of **62-iPr** could be improved from 43–66 h to 5 days.<sup>3</sup> Hazari and co-workers<sup>95</sup> showed that complex  $[\text{Fe}(\text{R}^{\text{P}}(\text{CH}_2)_2\text{N}(\text{CH}_2)_2\text{P})\text{H}(\text{CO})]$  **65-R** (R = iPr, cy; Fig. 24)

catalyzed the base-free dehydrogenation of methanol in water. Methyl formate was obtained as a side product, suggesting the incomplete dehydrogenation of methanol. Following the reaction by NMR revealed the formation of  $[\text{Fe}(\text{CyP}(\text{CH}_2)_2\text{NH}(\text{CH}_2)_2\text{P})\text{H}(\text{CO})(\text{OOCH})]$  (**66-cy**; Fig. 24), which took the catalyst away from the catalytic cycle. In the presence of a Lewis acid the accumulation of **66-cy** could be prevented. Thus, Lewis acids were used to promote the dehydrogenation of methanol. A TON of up to 51 000 could be reached.<sup>95</sup> In an analogous study, LiBF<sub>4</sub> was used to promote the dehydrogenation of formic acid catalyzed by **65-R** and **66-R** (R = iPr, cy). They obtained the best results using 0.0001 mol% of **66-iPr** in a 2.2% solution of formic acid in dioxane at 80 °C. 10 mol% of LiBF<sub>4</sub> was used as the additive. The reaction finished after 9.5 hours giving a TON of 983 642 with a TOF of 196 728 h<sup>-1</sup>.<sup>89</sup>



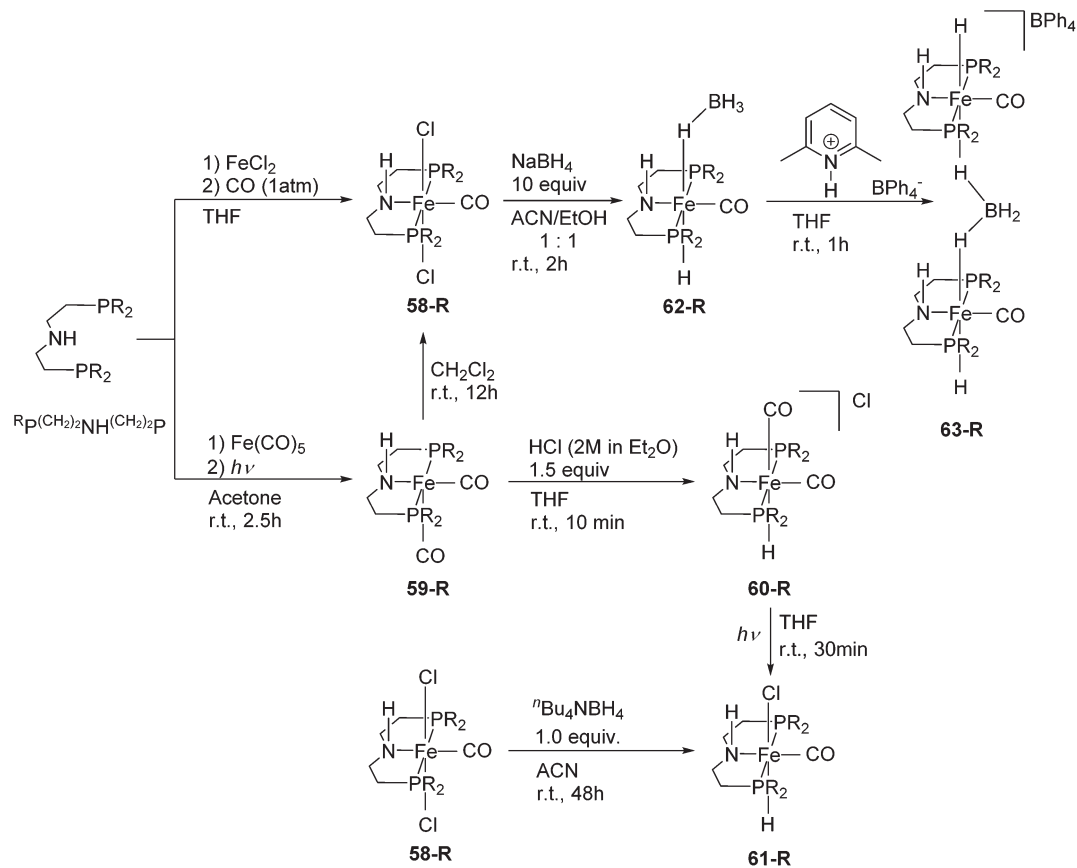


Fig. 23 Synthesis and reactivity of iron complexes of  $Rp(CH_2)_2NH(CH_2)_2P$ .

Table 13 Hydrogenation of nitriles and dinitriles catalyzed by complex **62-iPr**

Entry	Substrate	$T$ [ $^{\circ}C$ ]	Yield <sup>a</sup> [%]	Entry	Substrate	$T$ [ $^{\circ}C$ ]	Yield <sup>a</sup> [%]
1		70	97 <sup>b</sup>	13		100	80
2		70	99	14		130	92
3		100	81	15		100	40 <sup>b</sup>
4		70	84	16		100	58 <sup>b</sup>
5		70	92	17		130	75 <sup>c</sup>



Table 13 (Contd.)

$\begin{array}{c} \text{Ar}-\text{C}\equiv\text{N} \\ \text{or} \\ \text{N}\equiv\text{R}-\text{C}\equiv\text{N} \end{array} \xrightarrow[\text{T, 3h}]{\text{62-}i\text{Pr (1 mol\%)} \\ \text{iPrOH, 30 bar H}_2}$ $\begin{array}{c} \text{Ar}-\text{NH}_3^+ \text{Cl}^- \\ \text{or} \\ \text{Cl}^- \text{H}_3\text{N}-\text{R}-\text{NH}_3^+ \text{Cl}^- \end{array}$							
Entry	Substrate	T [°C]	Yield <sup>a</sup> [%]	Entry	Substrate	T [°C]	Yield <sup>a</sup> [%]
6		70	98	18		100	93
7		100	99	19		100	70
8		100	71	20		100	93
9		100	81	21		100 100	95 83 <sup>d</sup>
10		130	78	22		100	41
11		100	88	23		100	85
12		100	92				

<sup>a</sup> Isolated yields at full conversion (primary amines were isolated as HCl-salts). <sup>b</sup> GC-yield with hexadecane as the internal standard. <sup>c</sup> 10% transesterification product (–COO*i*Pr) product were observed. <sup>d</sup> Reaction was quenched after 20 min.

The groups of Schneider and Jones further reported the acceptorless dehydrogenation of different primary and secondary alcohols using **62-*i*Pr** as the catalyst.<sup>90</sup> The formed H<sub>2</sub> was removed from the reaction medium by a steady flow of N<sub>2</sub>, in order to shift the reaction equilibrium. Secondary benzylic alcohols (entries 1–8) were oxidized to the corresponding acetophenone derivatives in good to excellent yields (65–92%).

The protocol also tolerates a range of different functional groups (MeO, Me, NO<sub>2</sub> and halides). For substrates with electron withdrawing groups (entries 4–6) the catalyst loading could be lowered to 0.1 mol%. An aliphatic cyclohexanol (entry 10) was oxidized to cyclohexanone in a 64% yield. Primary alcohols and diols were also used as substrates. Benzylic alcohol formed benzyl benzoate exclusively (entry 9). The chemoselectivity of secondary over primary alcohol was tested using 1,2-propanediol and 1,3-butanediol (entries 13 and 14). In both cases the secondary hydroxyl group was oxidized before the primary group. The diols 1,2-benzenedimethanol and 1,5-pentanediol (entries 11 and 12) gave the corresponding lactones in 96 and 59% yield. Furthermore, it was shown that the reactions could be reversible, and the hydrogenation of ketones was achieved with **62-*i*Pr** as the catalyst (Table 14).<sup>93</sup>

Beller and co-workers further studied the dehydrogenation of diol substrates to give lactones catalyzed by **62-*i*Pr**.<sup>94</sup> In contrast to the conditions described by Schneider and Jones.<sup>90</sup> (toluene, reflux, 1 mol% **62-*i*Pr**), their reactions took place in

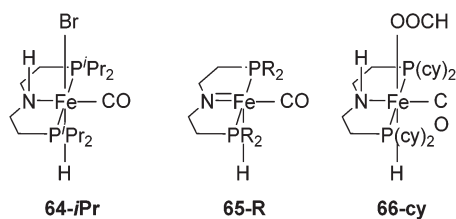
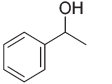
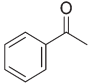
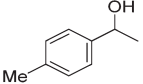
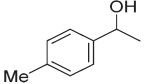
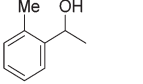
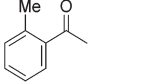
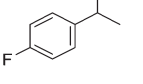
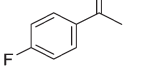
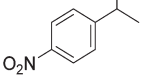
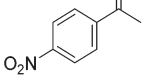
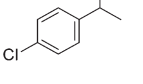
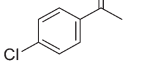
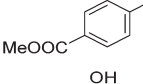
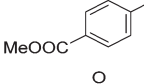
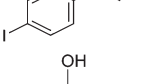
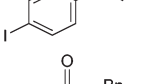
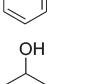
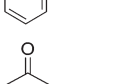
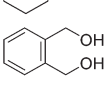
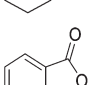
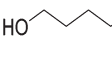
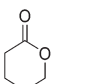
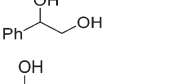
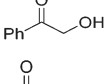
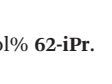

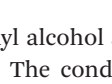
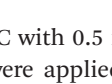


Fig. 24 Structure of complexes [Fe(*i*PrP(CH<sub>2</sub>)<sub>2</sub>NH(CH<sub>2</sub>)<sub>2</sub>P)H(CO)Br] (**64-*i*Pr**) and [Fe(RP(CH<sub>2</sub>)<sub>2</sub>N(CH<sub>2</sub>)<sub>2</sub>P)H(CO)] **65-R** (R = *i*Pr, cy).



**Table 14** Acceptorless dehydrogenation of alcohols catalyzed by **62-iPr**

Entry	Substrate	Product	Time [h]	Yield [%]
1			24	89
2			24	80
3			48	69
4			12 48 <sup>a</sup>	90 79 <sup>a</sup>
5			12 48 <sup>a</sup>	78 75 <sup>a</sup>
6			12 48 <sup>a</sup>	87 76 <sup>a</sup>
7			12	67
8			12	94
9			8	88
10			24	64
11			8	96
12			24	59
13			24	67
14			24	61

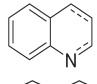
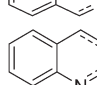
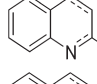
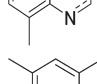
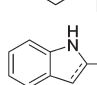
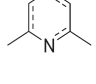


<sup>a</sup> 0.1 mol% **62-iPr**.

*tert*-amyl alcohol at 150 °C with 0.5 mol% **62-iPr** and 10 mol% K<sub>2</sub>CO<sub>3</sub>. The conditions were applied to 18 different aromatic and aliphatic diols which could be converted to the corres-

ponding 5-membered lactones in good to excellent yields. Also 6-membered and 7-membered lactones can be synthesized. The scope was further extended to 9 different  $\alpha,\omega$ -amino alcohols giving the corresponding lactams in good to excellent yields.

Jones and co-workers applied complexes **62-iPr**, **64-iPr** and **65-iPr** for the acceptorless dehydrogenation of saturated N-heterocycles to their aromatic counter parts and molecular H<sub>2</sub>.<sup>88</sup> The method was applied to a range of different 1,2,3,4-tetrahydroquinolines (Table 15, condition 1, entries 1–6). 2,6-Dimethylpiperidine and 2-methylindoline could be oxidized as well (entries 7 and 8). Partial dehydrogenation products were not observed. Remarkably, pyridine and quinoline products, which were potential ligands for iron, did not influence the reaction. It was observed that in the presence of 5 bar of H<sub>2</sub> **62-iPr** completely lost its catalytic activity for the dehydrogenation reaction, which suggested that this complex catalyzed the reverse reaction, the hydrogenation of unsaturated heterocycles in the presence of H<sub>2</sub>. This was indeed true, and con-

**Table 15** Reversible acceptorless dehydrogenation of N-heterocycles catalyzed by complexes **62-iPr** and **64-iPr**

Entry	N-heterocycle	Condition 1 Yield [%]	Condition 2 Yield [%]
1		69	77
2		72	66
3		91	92
4		83	n/a <sup>a</sup>
5		78	71
6		89	85
7		86	69
8		58	60

<sup>a</sup> Not accessible.

ditions were found for the hydrogenation of many such unsaturated heterocycles (Table 15, condition 2).

## 9. Summary and outlook

As described above, many new classes of iron pincer complexes have been recently synthesized and applied for organic synthesis. The reactivity of these complexes depends critically on the nature of the pincer ligands. The large number of successful applications underscores the advantages of pincer ligands, namely their diversity, modularity, and strong chelating ability. These examples also suggest that pincer ligands and iron catalysis are a perfect match for one another.

While iron pincer complexes are often used for hydrogenation, hydrosilylation, and related dehydrogenation reactions, their applications in other reactions including epoxidation, aziridation, and C–C bond-forming reactions are emerging. Given the many benefits of iron catalysis in organic synthesis, it is clear that there is a huge amount of unexplored potential of iron pincer complexes in catalysis. Until now, enantioselective catalysis using chiral iron pincer complexes remains scarce. This state will likely change rapidly in the near future.

## References

- B. Plietker, *Iron Complexes in Organic Chemistry*, Wiley-VCH Verlag GmbH & Co. KGaA, 2008.
- B. Plietker, *Iron Catalysis - Fundamentals and Applications*, Springer, Berlin Heidelberg, 2011.
- E. Alberico, P. Sponholz, C. Cordes, M. Nielsen, H.-J. Drexler, W. Baumann, H. Junge and M. Beller, *Angew. Chem., Int. Ed.*, 2013, **52**, 14162–14166.
- G. Van Koten, in *Organometallic Pincer Chemistry*, ed. G. Van Koten and D. Milstein, Springer, Berlin Heidelberg, 2013, vol. 40.
- D. Benito-Garagorri and K. A. Kirchner, *Acc. Chem. Res.*, 2008, **41**, 201–213.
- W. V. Dahlhoff and S. M. Nelson, *J. Chem. Soc. A*, 1971, 2184.
- C. J. Moulton and B. L. Shaw, *Dalton Trans.*, 1976, 1020.
- G. Van Koten, *Pure Appl. Chem.*, 1989, **61**, 1681–1694.
- B. Rybtchinski and D. Milstein, *Angew. Chem., Int. Ed.*, 1999, **38**, 870–883.
- C. M. Jensen, *Chem. Commun.*, 1999, 2443–2449.
- M. Albrecht and G. van Koten, *Angew. Chem., Int. Ed.*, 2001, **40**, 3750–3781.
- A. Vigalok and D. Milstein, *Acc. Chem. Res.*, 2001, **34**, 798–807.
- M. E. van der Boom and D. Milstein, *Chem. Rev.*, 2003, **103**, 1759–1792.
- D. Milstein, *Pure Appl. Chem.*, 2003, **75**, 445–460.
- J. T. Singleton, *Tetrahedron*, 2003, **59**, 1837–1857.
- B. L. Small, M. Brookhart and A. M. A. Bennett, *J. Am. Chem. Soc.*, 1998, **120**, 4049–4050.
- B. L. Small and M. Brookhart, *J. Am. Chem. Soc.*, 1998, **120**, 7143–7144.
- G. J. P. Britovsek, V. C. Gibson, B. S. Kimberley, P. J. Maddox, S. J. McTavish, G. A. Solan, A. J. P. White and D. J. Williams, *Chem. Commun.*, 1998, 849–850.
- G. J. P. Britoek, M. Bruce, V. C. Gibson, B. S. Kimberley, P. J. Maddox, S. Mastroianni, S. J. McTavish, C. Redshaw, G. A. Solan, S. Stromberg, A. J. P. White and D. J. Williams, *J. Am. Chem. Soc.*, 1999, **121**, 8728–8740.
- P. J. Chirik, in *Catalysis without Precious Metals*, Wiley-VCH Verlag GmbH & Co. KGaA, 2010, pp. 83–110.
- P. J. Chirik, in *Pincer and Pincer-Type Complexes*, Wiley-VCH Verlag GmbH & Co. KGaA, 2014, pp. 189–212.
- P. Giannoccaro, G. Vasapollo, C. F. Nobile and A. Sacco, *Inorg. Chim. Acta*, 1982, **61**, 69–75.
- J. Zhang, M. Gandelman, D. Herrman, G. Leitus, L. J. W. Shimon, Y. Ben-David and D. Milstein, *Inorg. Chim. Acta*, 2006, **359**, 1955–1960.
- R. J. Trovitch, E. Lobkovsky and P. J. Chirik, *Inorg. Chem.*, 2006, **45**, 7252–7260.
- E. M. Pelczar, T. J. Emge, K. Krogh-Jespersen and A. S. Goldman, *Organometallics*, 2008, **27**, 5759–5767.
- R. Langer, G. Leitus, Y. Ben-David and D. Milstein, *Angew. Chem., Int. Ed.*, 2011, **50**, 2120–2124.
- R. Langer, Y. Diskin-Posner, G. Leitus, L. J. W. Shimon, Y. Ben-David and D. Milstein, *Angew. Chem., Int. Ed.*, 2011, **50**, 9948–9952. The same group also reported a PNP–Fe complex with a new pyrazine-based pincer ligand and applied it for the hydrogenation of CO<sub>2</sub>, see: R. Langer, Y. Diskin-Posner, G. Leitus, L. J. W. Shimon, Y. Ben-David and D. Milstein, *Inorg. Chem.*, 2015, **54**, 4526.
- R. Langer, M. A. Iron, L. Konstantinovski, Y. Diskin-Posner, G. Leitus, Y. Ben-David and D. Milstein, *Chem. – Eur. J.*, 2012, **18**, 7196–7209.
- T. Zell, B. Butschke, Y. Ben-David and D. Milstein, *Chem. – Eur. J.*, 2013, **19**, 8068–8072.
- T. Zell, Y. Ben-David and D. Milstein, *Angew. Chem., Int. Ed.*, 2014, **53**, 4685–4689.
- T. Zell, Y. Ben-David and D. Milstein, *Catal. Sci. Technol.*, 2015, **5**, 822–826.
- D. Benito-Garagorri, E. Becker, J. Wiedermann, W. Lackner, M. Pollak, K. Mereiter, J. Kisala and K. A. Kirchner, *Organometallics*, 2006, **25**, 1900–1913.
- D. Benito-Garagorri, J. Wiedermann, M. Pollak, K. Mereiter and K. A. Kirchner, *Organometallics*, 2007, **26**, 217–222.
- D. Benito-Garagorri, L. G. Alves, M. Puchberger, K. Mereiter, L. F. Veiros, M. J. Calhorda, M. D. Carvalho, L. P. Ferreira, M. Godinho and K. A. Kirchner, *Organometallics*, 2009, **28**, 6902–6914.
- D. Benito-Garagorri, L. G. Alves, L. F. Veiros, C. M. Standfest-Hauser, S. Tanaka, K. Mereiter and K. A. Kirchner, *Organometallics*, 2010, **29**, 4932–4942.
- B. Bichler, C. Holzhaecker, B. Stöger, M. Puchberger, L. F. Veiros and K. A. Kirchner, *Organometallics*, 2013, **32**, 4114–4121.





- 37 B. Bichler, M. Glatz, B. Stöger, K. Mereiter, L. F. Veiros and K. A. Kirchner, *Dalton Trans.*, 2014, **43**, 14517–14519.
- 38 M. Glatz, B. Bichler, M. Mastalir, B. Stöger, M. Weil, K. Mereiter, E. Pittenauer, G. Allmaier, L. F. Veiros and K. A. Kirchner, *Dalton Trans.*, 2015, **44**, 281–294.
- 39 N. Gorgas, B. Stöger, L. F. Veiros, E. Pittenauer, G. Allmaier and K. A. Kirchner, *Organometallics*, 2014, **33**, 6905–6914.
- 40 W. S. DeRieux, A. Wong and Y. Schrodi, *J. Organomet. Chem.*, 2014, **772**, 60–67.
- 41 S. Mazza, R. Scopelliti and X. Hu, *Organometallics*, 2015, **34**, 1538–1545.
- 42 T. Zell and D. Milstein, *Acc. Chem. Res.*, 2015, **48**, 1979–1994.
- 43 C. R. Holmquist and E. J. Roskamp, *J. Org. Chem.*, 1989, **54**, 3258–3260.
- 44 S. J. Mahmood and M. M. Hossain, *J. Org. Chem.*, 1998, **63**, 3333–3336.
- 45 M. Redlich, S. J. Mahmood, M. F. Mayer and M. M. Hossain, *Synth. Commun.*, 2000, **30**, 1401–1411.
- 46 L. G. Alves, G. Dazinger, L. F. Veiros and K. A. Kirchner, *Eur. J. Inorg. Chem.*, 2010, 493160–493166.
- 47 G. Bauer and K. A. Kirchner, *Angew. Chem., Int. Ed.*, 2011, **50**, 5798–5800.
- 48 M. Albrecht, *Chem. Rev.*, 2010, **110**, 576–623.
- 49 P. Bhattacharya and H. R. Guan, *Comments Inorg. Chem.*, 2011, **32**, 88–112.
- 50 A. A. Kulkarni and O. Daugulis, *Synthesis*, 2009, 4087–4109.
- 51 C. S. Creaser and W. C. Kaska, *Inorg. Chim. Acta*, 1978, **30**, L325–L326.
- 52 P. Bhattacharya, J. A. Krause and H. R. Guan, *Organometallics*, 2011, **30**, 4720–4729.
- 53 S. Chakraborty, P. Bhattacharya, H. Dai and H. Guan, *Acc. Chem. Res.*, 2015, **48**, 1995–2003.
- 54 W. Wang, P. Gu, Y. Wang and H. Wei, *Organometallics*, 2014, **33**, 847–857.
- 55 P. Bhattacharya, J. A. Krause and H. R. Guan, *J. Am. Chem. Soc.*, 2014, **136**, 11153–11161.
- 56 P. Bhattacharya, J. A. Krause and H. R. Guan, *Organometallics*, 2014, **33**, 6113–6121.
- 57 D. F. Lu, C. L. Zhu, Z. X. Jia and H. Xu, *J. Am. Chem. Soc.*, 2014, **136**, 13186–13189.
- 58 H. Usuda, A. Kuramochi, M. Kanai and M. Shibasaki, *Org. Lett.*, 2004, **6**, 4387–4390.
- 59 M. Kawatsura, K. Kajita, S. Hayase and T. Itoh, *Synlett*, 2010, 1243–1246.
- 60 M. Nakanishi, A. F. Salit and C. Bolm, *Adv. Synth. Catal.*, 2008, **350**, 1835–1840.
- 61 A. Sharma and J. F. Hartwig, *Nature*, 2015, **517**, 600–604.
- 62 J. Jankowska, J. Paradowska and J. Mlynarski, *Tetrahedron Lett.*, 2006, **47**, 5281–5284.
- 63 J. Jankowska, J. Paradowska, B. Rakiel and J. Mlynarski, *J. Org. Chem.*, 2007, **72**, 2228–2231.
- 64 M. Kawatsura, Y. Komatsu, M. Yamamoto, S. Hayase and T. Itoh, *Tetrahedron Lett.*, 2007, **48**, 6480–6482.
- 65 M. Kawatsura, Y. Komatsu, M. Yamamoto, S. Hayase and T. Itoh, *Tetrahedron*, 2008, **64**, 3488–3493.
- 66 J. Wang, M. Frings and C. Bolm, *Chem. – Eur. J.*, 2014, **20**, 966–969.
- 67 H. Nishiyama and A. Furuta, *Chem. Commun.*, 2007, 760–762.
- 68 T. Chen, L. M. Yang, D. R. Gong and K. W. Huang, *Inorg. Chim. Acta*, 2014, **423**, 320–325.
- 69 Y. Imanishi and K. Nomura, *J. Polym. Sci., Part A: Polym. Chem.*, 2000, **38**, 4613–4626.
- 70 K. Nomura, W. Sidokmai and Y. Imanishi, *Bull. Chem. Soc. Jpn.*, 2000, **73**, 599–605.
- 71 A. M. Tondreau, J. M. Darmon, B. M. Wile, S. K. Floyd, E. Lobkovsky and P. J. Chirik, *Organometallics*, 2009, **28**, 3928–3940.
- 72 S. Hosokawa, J. Ito and H. Nishiyama, *Organometallics*, 2010, **29**, 5773–5775.
- 73 R. B. Bedford, M. Betham, D. W. Bruce, A. A. Danopoulos, R. M. Frost and M. Hird, *J. Org. Chem.*, 2006, **71**, 1104–1110.
- 74 R. P. Yu, J. M. Darmon, J. M. Hoyt, G. W. Margulieux, Z. R. Turner and P. J. Chirik, *ACS Catal.*, 2012, **2**, 1760–1764.
- 75 R. J. Trovitch, E. Lobkovsky, M. W. Bouwkamp and P. J. Chirik, *Organometallics*, 2008, **27**, 6264–6278.
- 76 D. Srimani, Y. Diskin-Posner, Y. Ben-David and D. Milstein, *Angew. Chem., Int. Ed.*, 2013, **52**, 14131–14134.
- 77 T. Niwa and M. Nakada, *J. Am. Chem. Soc.*, 2012, **134**, 13538–13541.
- 78 T. Inagaki, L. T. Phong, A. Furuta, J. Ito and H. Nishiyama, *Chem. – Eur. J.*, 2010, **16**, 3090–3096.
- 79 T. Inagaki, A. Ito, J. Ito and H. Nishiyama, *Angew. Chem., Int. Ed.*, 2010, **49**, 9384–9387.
- 80 G. Bauer, C. W. Cheung and X. Hu, *Synthesis*, 2015, 1726–1732.
- 81 G. Bauer, M. D. Wodrich, R. Scopelliti and X. Hu, *Organometallics*, 2015, **34**, 289–298.
- 82 Q.-H. Deng, T. Bleith, H. Wadepohl and L. H. Gade, *J. Am. Chem. Soc.*, 2013, **135**, 5356–5359.
- 83 T. Bleith, H. Wadepohl and L. H. Gade, *J. Am. Chem. Soc.*, 2015, **137**, 2456–2459.
- 84 W. Kuriyama, T. Matsumoto, O. Ogata, Y. Ino, K. Aoki, S. Tanaka, K. Ishida, T. Kobayashi, N. Sayo and T. Saito, *Org. Process Res. Dev.*, 2012, **16**, 166–171.
- 85 I. Köhne, T. J. Schmeier, E. A. Bielinski, C. J. Pan, P. O. Lagaditis, W. H. Bernskoetter, M. K. Takase, C. Würtele, N. Hazari and S. Schneider, *Inorg. Chem.*, 2014, **53**, 2133–2143.
- 86 S. Chakraborty, H. Dai, P. Bhattacharya, N. T. Fairweather, M. S. Gibson, J. A. Krause and H. Guan, *J. Am. Chem. Soc.*, 2014, **136**, 7869–7872.
- 87 S. Werkmeister, K. Junge, B. Wendt, E. Alberico, H. Jiao, W. Baumann, H. Junge, F. Gallou and M. Beller, *Angew. Chem., Int. Ed.*, 2014, **53**, 8722–8726.
- 88 S. Chakraborty, W. W. Brennessel and W. D. Jones, *J. Am. Chem. Soc.*, 2014, **136**, 8564–8567.



- 89 E. A. Bielinski, P. O. Lagaditis, Y. Zhang, B. Q. Mercado, C. Würtele, W. H. Bernskoetter, N. Hazari and S. Schneider, *J. Am. Chem. Soc.*, 2014, **136**, 10234–10237.
- 90 S. Chakraborty, P. O. Lagaditis, M. Förster, E. A. Bielinski, N. Hazari, M. C. Holthausen, W. D. Jones and S. Schneider, *ACS Catal.*, 2014, **4**, 3994–4003.
- 91 C. Bornschein, S. Werkmeister, B. Wendt, H. Jiao, E. Alberico, W. Baumann, H. Junge, K. Junge and M. Beller, *Nat. Commun.*, 2014, **5**, 4111.
- 92 N. T. Fairweather, M. S. Gibson and H. Guan, *Organometallics*, 2015, **34**, 335–339.
- 93 P. J. Bonitatibus Jr., S. Chakraborty, M. D. Doherty, O. Siclovan, W. D. Jones and G. L. Soloveichik, *Proc. Natl. Acad. Sci. U. S. A.*, 2015, **112**, 1687–1692.
- 94 M. Pena-Lopez, H. Neumann and M. Beller, *ChemCatChem*, 2015, **7**, 865–871.
- 95 E. A. Bielinski, M. Forster, Y. Zhang, W. H. Bernskoetter, N. Hazari and M. C. Holthausen, *ACS Catal.*, 2015, **5**, 2404–2415.

